Am J Transl Res 2020;12(9):5416-5432
www.ajtr.org /ISSN:1943-8141/AJTR0112847

Original Article

Assessment for prognostic value of differentially expressed genes in immune microenvironment of clear cell renal cell carcinoma

Xiaoxue Yin[1,2*], Xingming Zhang[3,4*], Zhenhua Liu[3,4*], Guangxi Sun[3,4], Xudong Zhu[3,4], Haoran Zhang[3,4], Sha Zhu[3,4], Jinge Zhao[3,4], Junru Chen[3,4], Pengfei Shen[3,4], Jia Wang[3,4], Ni Chen[1,2], Qiao Zhou[1,2], Hao Zeng[3,4]

*[1]Department of Pathology, [2]Institute of Pathology, [3]Department of Urology, [4]Institute of Urology, West China Hospital, Sichuan University, Chengdu 610041, P. R. China. *Co-first authors.*

Received April 19, 2020; Accepted August 1, 2020; Epub September 15, 2020; Published September 30, 2020

Abstract: Tumor-infiltrating immune cells have been recognized to be associated with prognosis and response to immunotherapy; however, genes related to immune microenvironment of clear cell renal cell carcinoma (ccRCC) remains unclear. To better understand the effects of genes involved in immune and stromal cells on prognosis, we used Cancer Genome Atlas Kidney Renal Clear Cell Carcinoma (TCGA-KIRC), DAVID database and ESTMATE algorithm, and divided the patients into low and high groups according to immune (median: 1038.45) and stromal scores (median: 667.945), respectively. We found the immune scores were significantly correlated with clinicopathological parameters and overall survival (OS). Based on immune scores, 890 DEGs were significantly associated with OS among the 1433 up-regulated genes. Based on top 10 DEGs (IL10RA, FCER1G, SASH3, TIGIT, RHOH, IL12RB1, AIF1, LPXN, LAPTM5 and SP140), cases with number of up-regulated genes ≥ 5 were associated poor OS ($P = 0.002$). In addition, the mean differences of percentages of CD8 T cells (11.32%), CD4 memory resting T cells (-4.52%) and mast resting cells (-3.55%) between low and high immune scores were the most significant. Thus, combination of these genes might use to predict the efficacy of immunotherapy. Further analyses of these genes were warrant to explore their potential association with the prognosis of ccRCC.

Keywords: Clear cell renal cell carcinoma, immune microenvironment, differentially expressed genes, prognosis

Introduction

Renal cell carcinoma (RCC) is one of the most common malignancies in urological oncology, and clear cell RCC (ccRCC), the most predominant histological type, accounts for more than 80% of RCCs [1]. Generally, ccRCC has been proved to be with highly infiltrated immune cells [2]. Meanwhile, approximate 1% spontaneous regression RCC, were attributed to immune-mediated [3]. Therefore, ccRCC was one of the earliest malignancies in history to be treated with immunotherapy, and heretofore remains one of the most responsive tumors [4-6]. In recent years, the progress of molecular immunology has promoted the discovery of immune checkpoint inhibitors (ICIs), which were successfully applied into clinical practice. Although complete response dramatically occurred up to 9% in patients with immunotherapy [7], still only part of population could benefit from either immunotherapy alone or immunotherapy combined with TKIs (ORR: 25-59%) [7-12]. Commonly speaking, response of ccRCC to immunotherapy was not satisfied as we expected [13]. And none of current biomarkers could determine immune infiltration and predict immunotherapy response [14]. This has prompted researchers around the world to keep exploring new potential biomarkers which can predict efficacy of immunotherapy and help clinical decision making.

In the context of immuno-oncology, growing evidences suggested that tumor microenvironment (TME) plays an important role in tumor progression, metastasis and therapeutic resistance [20, 21]. Immune and stromal cells are the two main types of non-tumor cells in TME [22]. It has been reported that regulatory T cells

(Tregs), tumor associated macrophages (TAM) and CD8$^+$ T cells have different effects on tumor cells [23-27]. Meanwhile, multiple researches have demonstrated that immune microenvironment is closely related to ccRCC [28-30]. Whereas, the mechanisms of TME highly infiltrated with immune cells, spontaneous tumor remission in the course of treatment of primary tumor and the treatment response to immunotherapy in ccRCC still remain obscure. Since the immune microenvironment is a complex space consisted of various kinds of immune cells, identification of these cells alone is insufficient to assess the complex microenvironment. Considering the limitations of technique, such as the difficulty to simultaneously assess the number of miscellaneous cell types and the high demanded amount of tissue, Yoshihara et al. designed a calculation to quantitatively predict immune and stromal scores based on ESTIMATE algorithm (Estimation of STromal and Immune cells in MAlignant Tumor tissues using Expression data), which utilizes specific genes in immune and stromal cells to predict scores of tumor purity and infiltration extent [31, 32].

The cancer genome atlas (TCGA) is an open database aims to apply high-throughput genomic sequencing techniques to assist better understanding of cancer and thus improve the ability to prevent, diagnose and treatment of cancer [33, 34]. In order to analyze the influences of immune and stromal related genes on the prognosis of ccRCC, we aimed to classify ccRCC cases of TCGA into low and high score groups based on immune and stromal scores. Subsequently, we planned to identify differentially expressed genes between low and high groups and to screen the most significant genes to predict outcomes of ccRCC.

Materials and methods

Acquisition of gene expression profile data

We obtained level 3 gene expression profile of ccRCC patients (KIRC) from the TCGA data portal (https://tcga-data.nci.nih.gov/tcga/). In addition, clinical and pathological data were also downloaded. The presence of infiltrating stromal/immune cells in tumor tissues of ccRCC was predicted by a tool of ESTIMATE algorithm created by Yoshihara et al.

Relationship between immune/stromal score and clinicopathological parameters and overall survival (OS)

Based on the immune/stromal scores mentioned before, we classified cases of ccRCC into low and high groups by medians according to immune and stromal scores, respectively. Subsequently, we analyzed correlations between immune or stromal scores and T stage, histologic type, tumor stage and top 4 mutated genes in ccRCC (VHL, PBRM1, SETD2 and BAP1). We used non-parametric test to analyze differences between low and high group. Additionally, survival analysis using log rank test was conducted to assess difference between low and high groups of immune/stromal scores, and Kaplan-Meier curves were plotted by R software.

Identification of differentially expressed genes (DEGs) between low and high groups stratified by immune or stromal scores

DEGs between low and high groups were identified by performing data analysis according to limma package from R software [35]. The following cut-off points were adopted to screen DEGs: > 1.5 of fold change with adjusted P value < 0.05. Heatmaps, volcano plot and venn diagram were plotted by R software using pheatmap package, ggplot2 and gplots.

Functional enrichment analysis of DEGs

DAVID (The Database for Annotation, Visualization and Integrated Discovery) is a classic database (https://david.ncifcrf.gov/) mainly used for gene functional enrichment analysis [36]. DAVID provides a comprehensive annotation of biological function, and we used the database to conduct gene ontology (GO) functional annotation and Kyoto encyclopedia of genes and genomes (KEGG) pathway analysis. GO annotation included three parts: biological process (BP), molecular function (MF) and cell composition (CC). Visual results of the above analysis were presented by bubble plot conducted by using R software with ggplot2 package. P value < 0.05 was considered as cut-off point of statistically significant.

Construction of protein-protein interaction (PPI) network and module analysis

We used a biological database named STRING (Search Tool for the Retrieval of Interacting

Genes) for PPI analysis. The role of the database (http://string.embl.de/) was to conduct a network of PPI for identified DEGs on the basis of the proven and predicted PPIs, and then analyze the potential interactions among proteins [37]. After online analysis, TSV format files were downloaded for further analysis in Cytoscape software (version 3.5.1) [38]. We used Cytoscape software to visualize PPI network and explore top 3 significant modules of network with 10 or more nodes.

Survival analysis

Analysis of overall outcome was performed by R software with survival package. Additionally, Kaplan-Meier plots were conducted by R software with survminer package. We calculated hazard ratio (HR) and log-rank *P* value for presentation. *P* value < 0.05 was considered as cut-off point of statistically significant.

The composition differences of 22 immune cell subtypes between low and high immune scores

In order to quantify the abundance of 22 immune subtypes in ccRCC specimens, the CIBERSORT deconvolution algorithm was applied [39]. Specifically, gene expression data was uploaded to the CIBERSORT web portal (http://cibersort.stanford.edu/) to calculate proportions of immune cells using the LM22 signature at 1,000 permutations. After acquisition of the infiltration data of each case, we planned to find the difference of abundance of immune infiltration cells between low and high groups of immune scores.

Oncomine and clinical proteomic tumor analysis consortium (CPTAC) database analysis

In this study, we tried to validate the mRNA and protein expression of top 10 DEGs based on two existing cancer database: Oncomine (https://www.oncomine.org/) and CPTAC (http://ualcan.path.uab.edu/analysis-prot.html). Filters of Oncomine database were set: primary filters were set as differential analysis (cancer versus normal tissue) and cancer type (clear cell renal cell carcinoma). Data type was set as mRNA, then differential expression of mRNA between ccRCC and normal tissue was displayed. For CPTAC, Z-values represent standard deviations from the median across samples for the given cancer type. Log2 Spectral count ratio values from CPTAC were first normalized within each sample profile, then normalized across samples.

Results

Immune scores were significantly correlated with clinicopathological parameters and OS

Among all 537 cases downloaded from TCGA portal, 191 (35.6%) cases were female, 346 (64.4%) cases were male. The median age was 61 y (ranged from 26 to 90 y). According to ESTIMATE algorithm mentioned before, the distributions of immune and stromal scores were ranged from -11.57.91 to 2030.4 and from 1158.94 to 3076.4, respectively. As presented in **Figure 1**, cases with T stage ≥ 2 were associated with higher immune scores rather than stromal scores (**Figure 1A**, **1B**). Tumor stage was not statistically different in both immune and stromal scores (**Figure 1C**, **1D**). For histological grade, immune scores increased with escalation of nuclear grade (**Figure 1E**), whereas no such trend was observed in stromal scores (**Figure 1F**).

Four top mutated genes, including VHL, PBRM1, SETD2 and BAP1, were observe from the TCGA.I Immune scores were correlated with mutations of BAP1 while stromal scores were not statistically associated with all four genes (**Figure 1G-N**). We further analyzed the correlations of immune and stromal scores with OS, and Kaplan-Meier survival curves showed that cases with high immune scores were associated poorer OS (**Figure 1O**), whereas stromal scores were not correlated with OS (**Figure 1P**).

Gene expression profiles were distinct between the low and high groups stratified by immune and stromal scores. As shown in **Figure 2A-C**, the gene expression profiles presented by RNAseq data were significantly different between low and high groups in both immune and stromal scores. Based on immune scores, a total of 1433 genes were up-regulated and 1910 genes were down-regulated. For stromal scores, the numbers of up-regulated and down-regulated genes were 230 and 235, respectively. The numbers of up-regulated and down-regulated genes in both immune and stromal

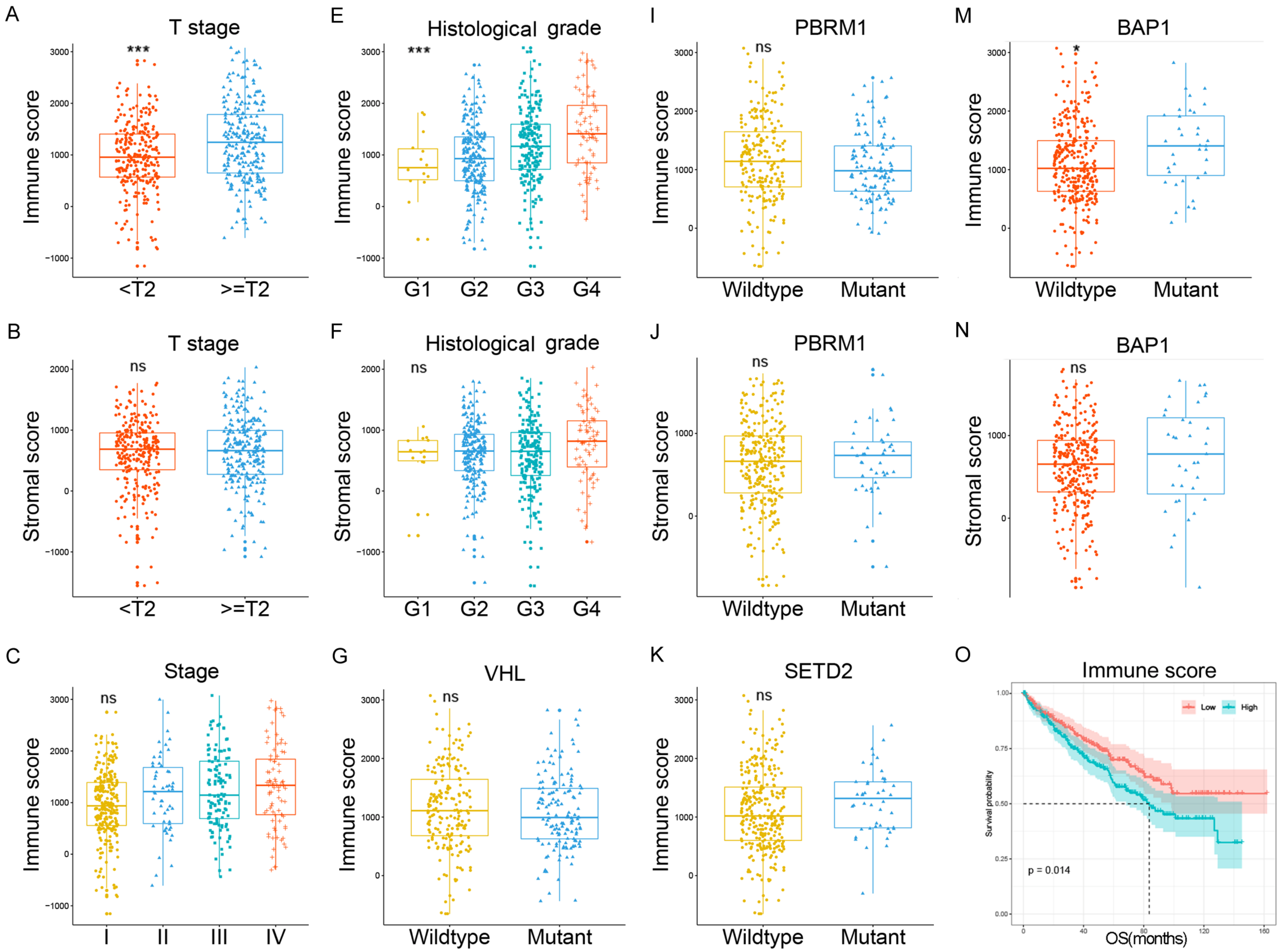
A
T stage
Immune score
***
<T2
>=T2
E
Histological grade
Immune score
***
G1
G2
G3
G4
I
PBRM1
Immune score
ns
Wildtype
Mutant
M
BAP1
Immune score
*
Wildtype
Mutant
B
T stage
Stromal score
ns
<T2
>=T2
F
Histological grade
Stromal score
ns
G1
G2
G3
G4
J
PBRM1
Stromal score
ns
Wildtype
Mutant
N
BAP1
Stromal score
ns
C
Stage
Immune score
ns
I
II
III
IV
G
VHL
Immune score
ns
Wildtype
Mutant
K
SETD2
Immune score
ns
Wildtype
Mutant
O
Immune score
Low
High
Survival probability
p = 0.014
OS(months)
0
40
80
120
160
0.00
0.25
0.50
0.75
1.00
3000
2000
1000
0
−1000

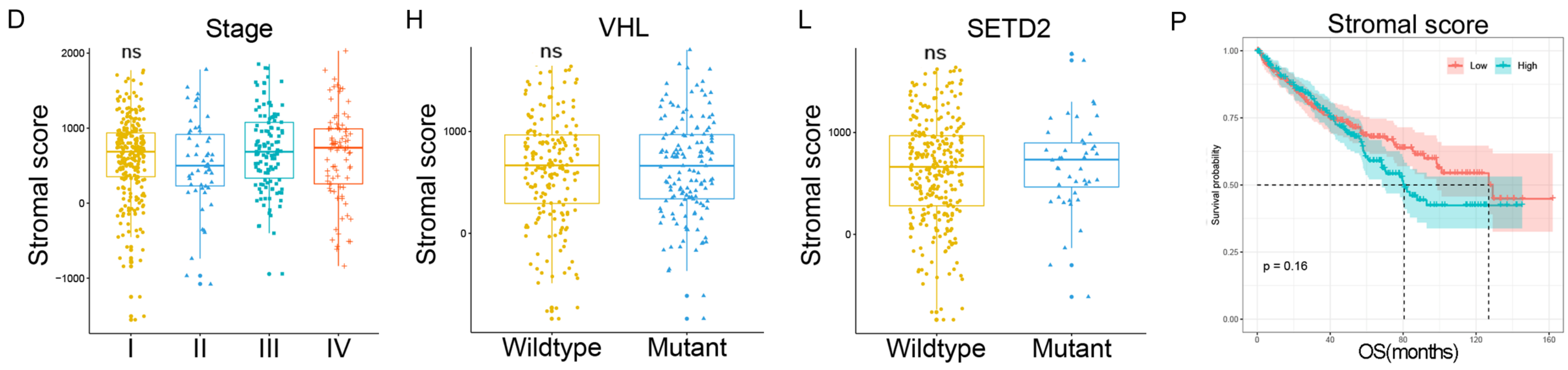

Figure 1. Immune scores were significantly correlated with clinicopathological parameters and OS. (A and B) Represented the associations of T stage with immune and stromal scores, cases with T stage ≥ 2 were associated with higher immune score rather than stromal score. (C and D) Showed there were no relationship between tumor stage and immune or stromal scores. (E and F) Indicated immune scores were increased with escalation of nuclear grade, but no such trend was observed in stromal scores. From (G-N), correlations of top 4 mutated genes of TCGA with immune and stromal scores were presented. Except for BAP1, immune scores were not correlated with mutations of VHL, PBRM1 and SETD2, while stromal scores were not statistically associated with all four genes. We further analyzed the correlations of immune and stromal scores with OS. (O and P) Showed Kaplan-Meier survival curves of immune and stromal scores for OS.

scores were 722 and 77, respectively (**Figure 2D**, **2E**).

It is worth noting that DEGs identified from low and high groups are relatively independent between immune scores and stromal scores. And based on the prognosis results of immune and stromal scores (**Figure 1O**, **1P**), stromal scores had no value in predicting prognosis. Therefore, we conducted all subsequent analysis based on DEGs identified from immune scores in the present study. Functional enrichment analysis of the 1433 up-regulated genes revealed that these genes were mainly involved in the biological process of immune and inflammatory response (**Figure 2F**), the cellular components of plasma membrane (**Figure 2G**), the molecular function of carbohydrate binding (**Figure 2H**) and the KEEG pathway of cytokine-cytokine receptor interaction (**Figure 2I**).

Individual DEGs and OS

We explored the relationships of the 1433 up-regulated genes to OS and a total of 890 DEGs were statistically significant (Table S1). Among them, 855 genes were shown to predict poor OS and only 35 genes were shown to predict favorable OS. Kaplan-Meir survival curves of selected genes (Top 10 DEGs) were shown in **Figure 3** and high expression of each gene was associated with poor OS.

PPI network among prognostic DEGs

We obtained the protein-protein interaction among DEGs by using the STRING tool. After downloading the data, we plotted PPI network through Cytoscape software for subsequent analysis. The whole network was composed of 733 nodes and 7001 edges, and a total of 7 modules were screened through MCODE. For further analysis, we selected the three most important modules (**Figure 4**). In the module 1, a total of 32 nodes and 495 edges form the network, and CXCL8, CXCR3/4/5 and CCL4/5 were the most important nodes (**Figure 4A**). In the module 2 (**Figure 4B**), 55 nodes involving 639 edges were formed in the network. The main nodes included IL6, IL10, CTLA4, FOXP3, and ITGAX. The module 3 was consisted of 47 nodes and 297 edges, including MMP9, STAT1, IL10RA and CD80 as the most important nodes (**Figure 4C**). To describe the types of proteins in the PPI network in terms of immune microenvironment, we additionally presented each protein's extracellular/subcellular locations (secreted, extracellular and cell surface proteins), and its function (Table S2). Specifically, module 1 and module 3 were characterized as secreted or membrane proteins, as these proteins accounted for 93.8% (30/32) and 70.2% (33/47) of the whole network, respectively. For module 2, most proteins were classified into intracellular (58.2%, 32/55).

Functional enrichment analysis of DEGs with prognostic value and the role of top 10 hub genes in predicting OS. Functional enrichment analysis of the 890 DEGs revealed that these genes were mainly involved in immune and inflammatory response (**Figure 5A**), plasma membrane (**Figure 5B**), carbohydrate binding (**Figure 5C**) and cytokine-cytokine receptor interaction (**Figure 5D**), which were identical to the results of the 1433 up-regulated genes and PPI network analysis.

We further classified cases into two groups based on number of up-regulated genes in Top 10 DEGs (IL10RA, FCER1G, SASH3, TIGIT, RHOH, IL12RB1, AIF1, LPXN, LAPTM5 and SP140). **Figure 5E** showed the heatmap of these genes between low and high immune score groups. Kaplan-Meir survival curve was plotted to verify the prognostic value of the classification. Cases with number of up-regulated genes ≥ 5 were associated poor OS ($P = 0.002$, **Figure 5F**).

The compositions of CD8 T cells, CD4 memory resting T cells and mast resting cells were significant different between low and high immune scores. Among 22 subtypes of immune infiltration cells, up to 72.7% (16/22) of cells were statistically different between low and high immune scores (**Figure 6**). The mean differences of percentages of CD8 T cells (11.32%), CD4 memory resting T cells (-4.52%) and mast resting cells (-3.55%) between low and high immune scores were the most significant, with CD8 T cells the greatest (increased from 7.64% to 18.96%, $P < 0.001$). It is noteworthy that the trend of change in cell composition of CD8 T cells were opposite to CD4 memory resting T cells and mast resting cells (**Figure 6**).

Validation of DEGs

We further validated top 10 DEGs in patients from Oncomine and CPTAC database. As shown in Table S3, only LPXN was not differentially

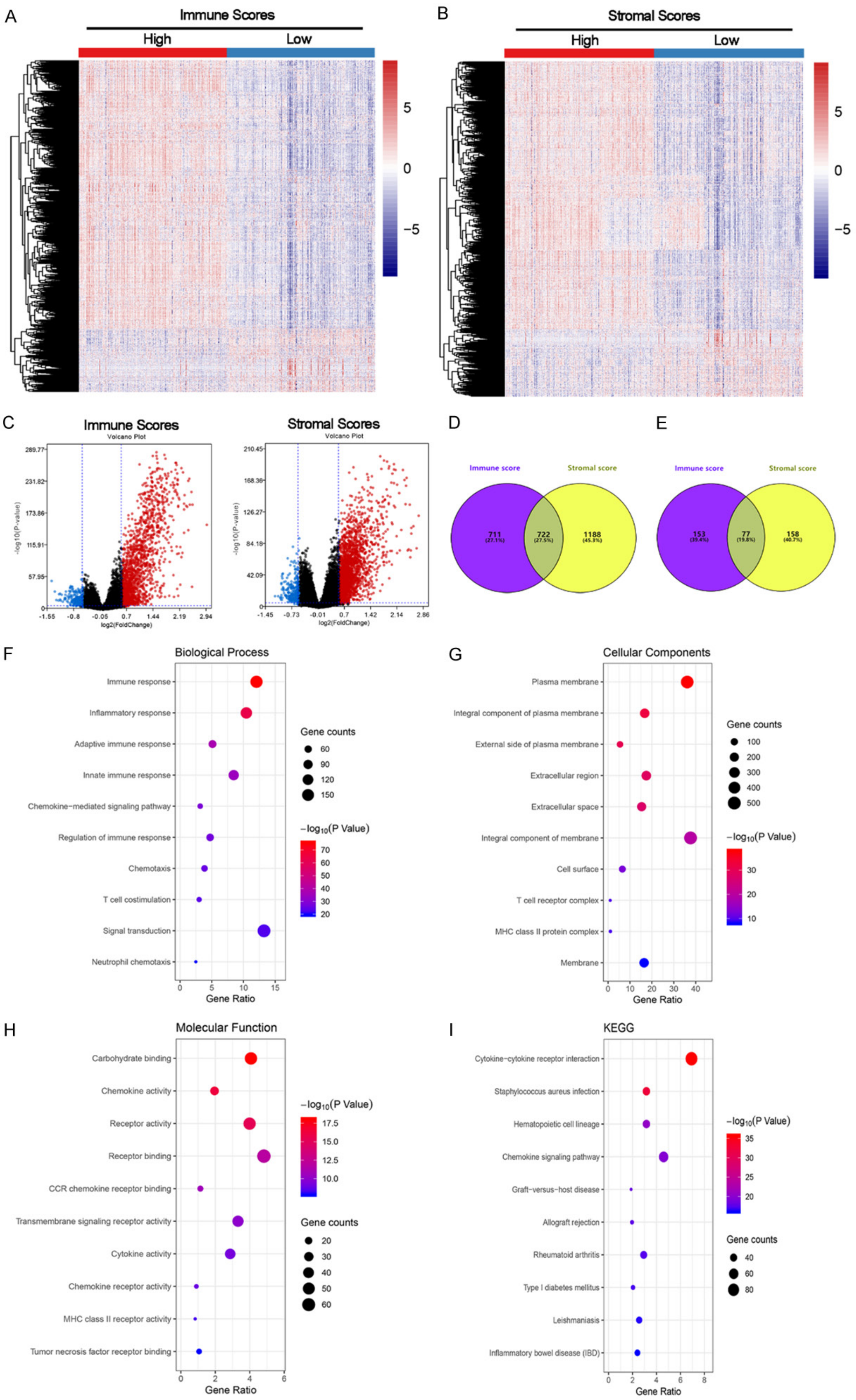
A
Immune Scores
High
Low
5
0
−5
B
Stromal Scores
High
Low
5
0
−5
C
Immune Scores
Volcano Plot
-log10(P-value)
289.77
231.82
173.86
115.91
57.95
0
-1.55
-0.8
-0.05
0.7
1.44
2.19
2.94
log2(FoldChange)
Stromal Scores
Volcano Plot
-log10(P-value)
210.45
168.36
126.27
84.18
42.09
0
-1.45
-0.73
-0.01
0.7
1.42
2.14
2.86
log2(FoldChange)
D
Immune score
Stromal score
711 (27.1%)
722 (27.5%)
1188 (45.3%)
E
Immune score
Stromal score
153 (39.4%)
77 (19.8%)
158 (40.7%)
F
Biological Process
Immune response
Inflammatory response
Adaptive immune response
Innate immune response
Chemokine−mediated signaling pathway
Regulation of immune response
Chemotaxis
T cell costimulation
Signal transduction
Neutrophil chemotaxis
0
5
10
15
Gene Ratio
Gene counts
60
90
120
150
−log10(P Value)
70
60
50
40
30
20
G
Cellular Components
Plasma membrane
Integral component of plasma membrane
External side of plasma membrane
Extracellular region
Extracellular space
Integral component of membrane
Cell surface
T cell receptor complex
MHC class II protein complex
Membrane
0
10
20
30
40
Gene Ratio
Gene counts
100
200
300
400
500
−log10(P Value)
30
20
10
H
Molecular Function
Carbohydrate binding
Chemokine activity
Receptor activity
Receptor binding
CCR chemokine receptor binding
Transmembrane signaling receptor activity
Cytokine activity
Chemokine receptor activity
MHC class II receptor activity
Tumor necrosis factor receptor binding
0
2
4
6
Gene Ratio
−log10(P Value)
17.5
15.0
12.5
10.0
Gene counts
20
30
40
50
60
I
KEGG
Cytokine−cytokine receptor interaction
Staphylococcus aureus infection
Hematopoietic cell lineage
Chemokine signaling pathway
Graft−versus−host disease
Allograft rejection
Rheumatoid arthritis
Type I diabetes mellitus
Leishmaniasis
Inflammatory bowel disease (IBD)
0
2
4
6
8
Gene Ratio
−log10(P Value)
35
30
25
20
Gene counts
40
60
80

Figure 2. Gene expression profiles were distinct between low and high groups stratified by immune and stromal scores. A-C. Showed that the gene expression profiles were significantly different between low and high groups in both immune and stromal scores. Based on immune scores, a total of 1433 genes were up-regulated and 1910 genes were down-regulated. For stromal scores, the numbers of up-regulated and down-regulated genes were 230 and 235, respectively. D and E. Represented numbers of genes up-regulated or down-regulated genes in both immune and stromal scores. F-I. Indicated functional enrichment analysis of the 1433 up-regulated genes. These genes were mainly involved in the biological process of immune and inflammatory response, the cellular components of plasma membrane, the molecular function of carbohydrate binding and the KEEG pathway of cytokine-cytokine receptor interaction.

expressed between clear cell renal cell carcinoma and normal tissue, with other 9 genes observed with higher mRNA expression in carcinoma than normal tissue. For protein expression, data of 6 DEGs were found in the CPTAC database, and all were over-expressed in the carcinoma compared to normal tissue, except for RHOH (Figure S1).

Discussion

As the in-depth research on molecular mechanism of incidence and evolution of solid tumors including renal cell carcinoma, ICIs were used to block co-inhibitory signals, prevent inactivation of T cells and then facilitate T cells to kill tumor cells [40, 41]. The unsatisfied treatment response keeps impelling researchers concentrate on developing and optimizing biomarkers. Current biomarkers focusing on immune status and prognostic models were not sufficient in screening out appropriate patients to receive ICIs treatment. Thus, it is important to focus on the comprehensive immune status in TME. Based on this, we aimed to predict the prognosis of ccRCC by calculating immune and stromal scores in the aspect of comprehensive level, and explore potential immune related genes to predict prognosis of ccRCC.

In the present study, we found that immune score was a poor prognostic factor of OS. Since stromal score was not associated with prognosis, all subsequent analysis was based on immune score. After comparing gene expression profiles of cases with low and high scores, a total of 1433 genes related to immune response were identified. Functional enrichment analysis showed that most of these genes were involved in tumor microenvironment. Further survival analysis revealed that 890 genes were found to be associated with prognosis, and PPI network analysis also found that these genes were associated with immune or inflammatory responses, such as IL6, IL10, CTLA4, FOXP3, and ITGAX in module 1. We further presented proteins location for these differentially expressed genes were analyzed by using immune microenvironment score. The results showed that module 1 and model 3 were characterized by secreted and membrane proteins, and module 2 was mainly consisted by intracellular proteins. This might provide potential hints for future research on mechanism of immune microenvironment and provide insights into improvement of the prediction and efficacy of immunotherapy in oncology. Eventually, we identified top 10 prognosis-related DEGs to be integrated as one comprehensive parameter to predict prognosis of ccRCC, which were IL10RA, FCER1G, SASH3, TIGIT, RHOH, IL12RB1, AIF1, LPXN, LAPTM5 and SP140. Kaplan-Meier survival analysis suggested that patients with number of up-regulated genes ≥ 5 have shorter OS compared to patients with number of up-regulated genes < 5.

The top 10 prognosis-related DEGs were found to be mainly correlated with immune and inflammatory process. IL10RA (Interleukin 10 Receptor Subunit Alpha) was mainly expressed on most hematopoietic cells and functioned as anti-inflammatory factor [42, 43]. FCER1G (Fc Fragment Of IgE Receptor Ig) was associated with allergic reactions and played a role in tumor development and squamous carcinogenesis [44, 45]. In addition, FCER1G was associated with progression and prognosis of ccRCC [46]. Mutations or abnormal expressions of SASH3 (SAM And SH3 Domain Containing 3), RHOH (Ras Homolog Family Member H), LPXN (leupaxin) and LAPTM5 (lysosomal protein transmembrane 5) have been demonstrated to be associated with the development and progression multiple malignancies [47-56]. TIGIT (T cell immunoglobulin and ITIM domain), IL12RB1 (Interleukin 12 Receptor Subunit Beta 1), AIF1 (allograft inflammatory factor 1) and SP140 (SP140 nuclear body protein) mainly involved in the process of immune and inflam-

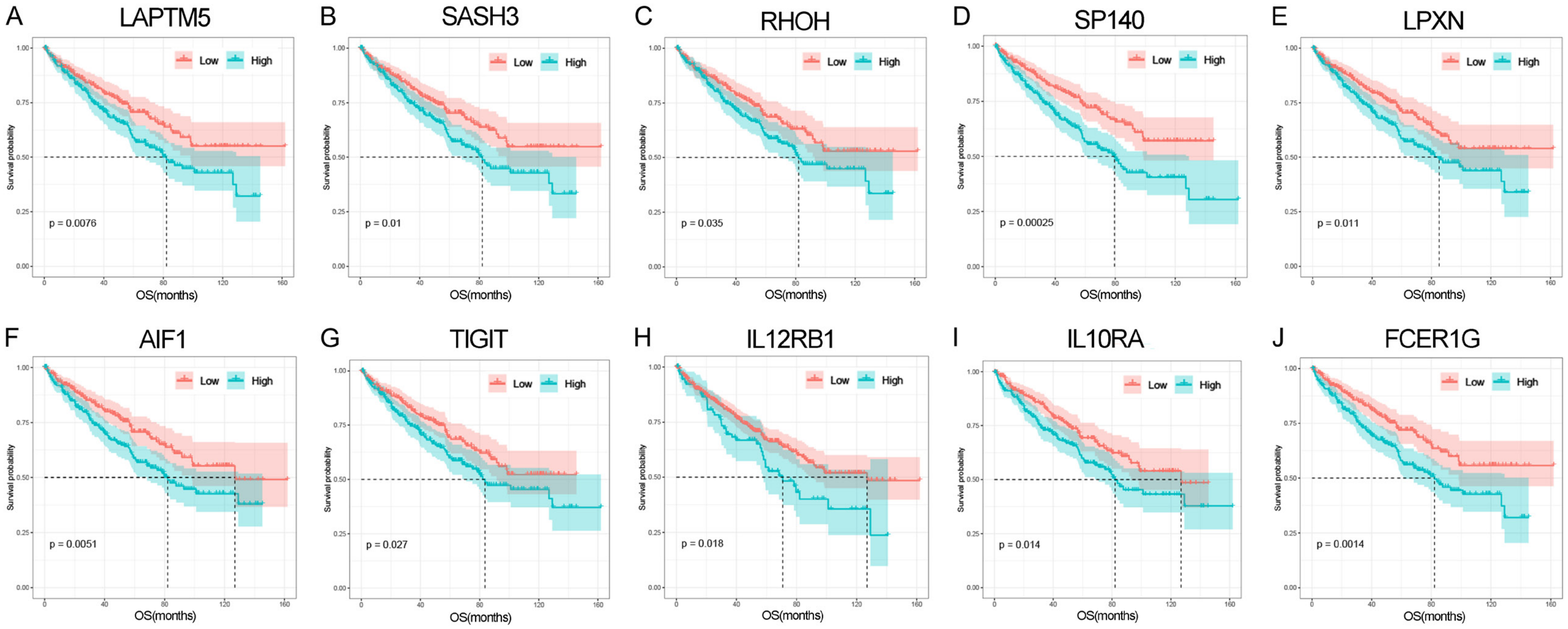

Figure 3. Associations of top 10 individual DEGs with OS. (A-J) Showed the relationship of top 10 DEGs and OS. Patients were divided into two groups (low and high) according to median mRNA expression of each gene. As shown in the figure, all genes were statistically associated with OS, and all genes were associated with unfavorable survival. All patients with high expression stratified by top 10 DEGs reached median OS, and only patients with high expression of AIF1, IL12RB1 and IL10RA reached median OS (F, H and I).

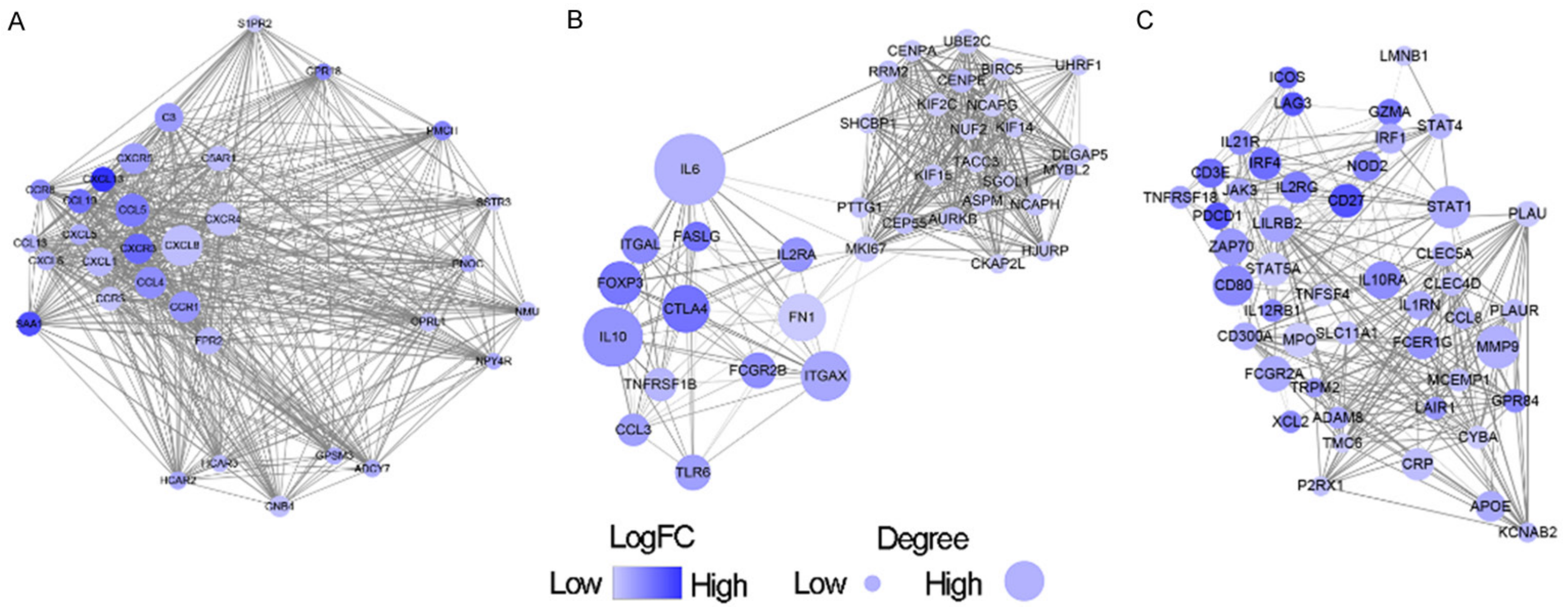

Figure 4. PPI network among prognostic DEGs. A. Represented module 1, consisted of 32 nodes and 495 edges. B. Represented module 2, formed by 55 nodes and 639 edges. C. Represented module 3, involving 47 nodes and 297 edges.

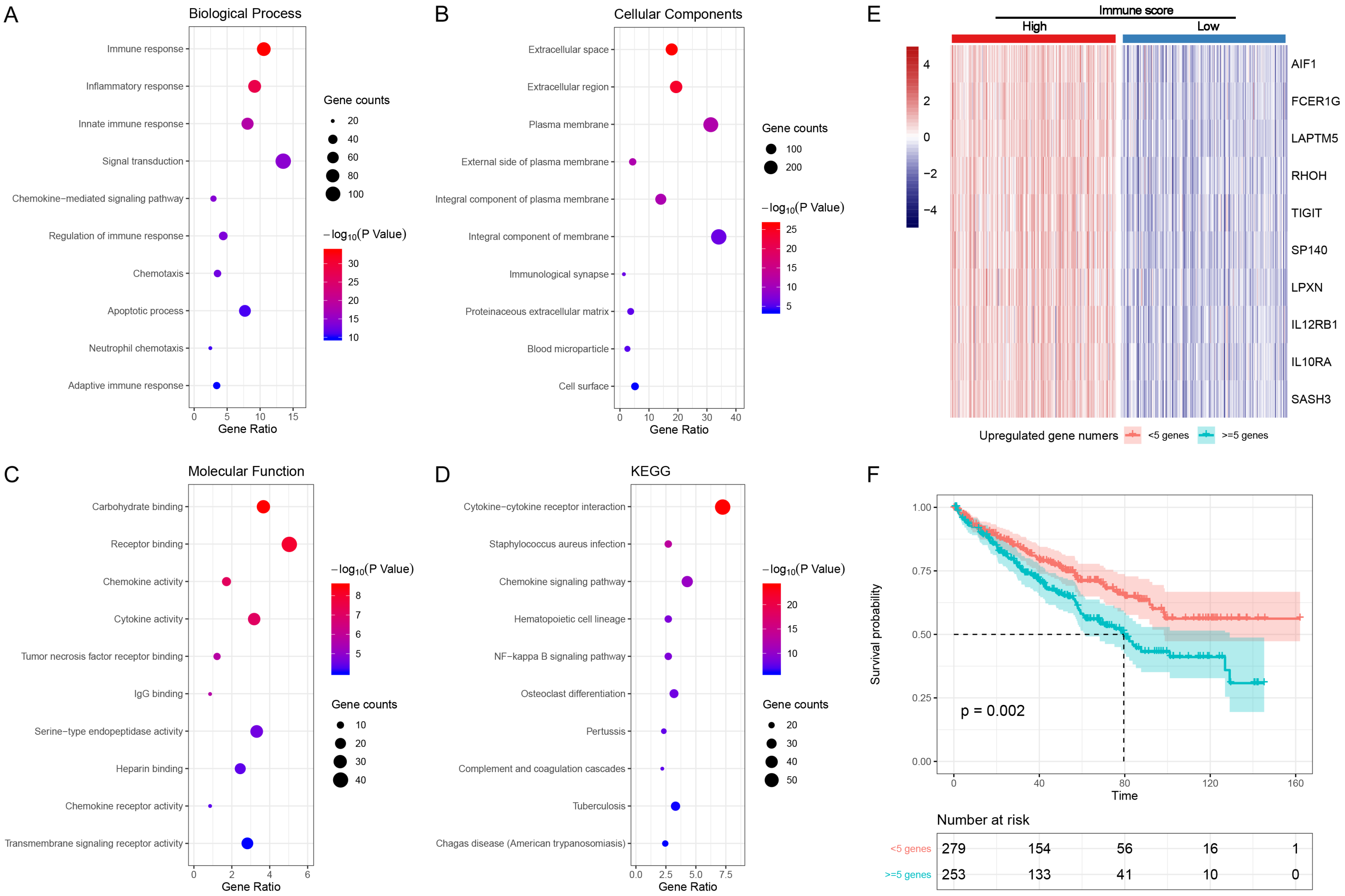

<5 genes	279	154	56	16	1
>=5 genes	253	133	41	10	0

Figure 5. Functional enrichment analysis of DEGs with prognostic value and the role of top 10 hub genes in predicting OS. (A-D) Represented functional enrichment analysis, these genes were mainly involved in immune and inflammatory response, plasma membrane, carbohydrate binding and cytokine-cytokine receptor interaction. (E) Represented the heatmap of these genes between low and high immune score groups and (F) represented Kaplan-Meir survival curve of OS in cases classified by number of up-regulated genes ≥ 5 or not.

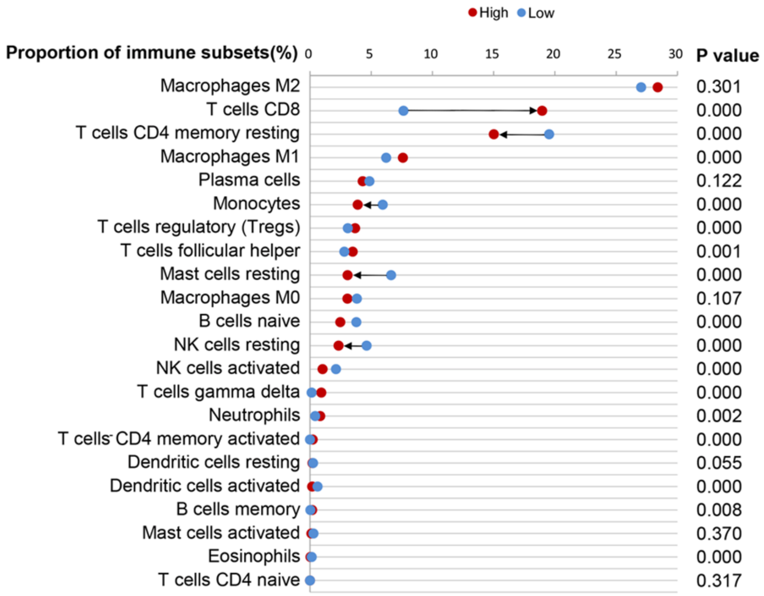

Figure 6. The compositions of cells in the immune microenvironment between low and high immune scores. The compositions of CD8 T cells, CD4 memory resting T cells and mast resting cells were significant different between low and high immune scores (arrow).

mation. As a novel immune checkpoint receptor similar to PD-1, TIGIT is upregulated on CD8+ TILs and Tregs in multiple tumors, exhibiting therapeutic benefits in animal models [57, 58]. IL12RB1 promotes delayed type hypersensitivity and autoimmunity [59]. AIF1 is mainly associated with allograft rejection, autoimmune diseases and vasculopathy, etc. [60]. SP140 was demonstrated to be associated with multiple sclerosis [61].

We also compared subtypes of immune cells between low and high immune scores to find potential factors attributed to the situation of high immune score. It seemed that increased compositions of CD8 T cells and decreased proportions of CD4 memory resting T cells and mast resting cells were the most important in contributing to higher immune score. Therefore, the higher immune score, the worse prognosis may be mainly related to CD8 T cells, which is consistent with previous research evidence, suggesting that the reactions of immune cells were more pronounced as the progression of tumor grade/biological malignancy, possibly due to the increased antigenicity of tumor cells [62, 63].

Immunohistochemistry (IHC), flow cytometry (FCM) and next-gene sequencing (NGS) were the three major tools to assess immune status. Previous reports about immune status and prognosis were mainly based on IHC and FCM, which focused on single or partial subtypes of immune cells [64-66]. It has been found that immune scores (scored by densities of $CD3^+$ and $CD8^+$ by IHC) can accurately estimate the risk of recurrence in colon cancer, and these results support the inclusion of immune scores as a new component of the TNM immune cancer classification [67]. In terms of ccRCC, Kawashima et al. classified patients' immune status into 3 groups using 5 markers (PD-1, TIM-3, ICOS, CD45RA, and CD-25). The classification of the above 3 groups was significantly associated with tumor grade [68]. Theoretically, the prediction of immunotherapy efficacy based on molecular markers of tumor and/or immune cells alone is not comprehensive and the clinical effect is mostly not satisfactory. ICIs are different from antiangiogenic drugs in that they act directly on tumor microenvironment rather than tumor cells. Therefore, a growing number of researchers are focusing on the predictive value of comprehensive evaluation. In the field of ccRCC, efforts have been made in characterizing immune status in a more comprehensive way. Xu et al. has developed novel signatures of immune infiltration based on calculating immune and stromal scores [69]. In the present study, we identified top 10 immune microenvironment-related genes and these genes were integrated into one parameter to represent immune status. Survival analysis demonstrated that this integrated parameter can distinguish patients with good or poor prognosis. However, further researches are warrant to explore the potential of predictive value of these genes in the immunotherapy of ccRCC.

Acknowledgements

This work was supported by Natural Science Foundation of China (NSFC 81974398, 819-02577 and 81672547) and 1.3.5 project for disciplines of excellence, West China Hospital, Sichuan University (No.0040205301E21).

Disclosure of conflict of interest

None.

Abbreviations

ccRCC, clear cell renal cell carcinoma; DEGs, differentially expressed genes; ICIs, immune checkpoint inhibitors; TME, tumor microenvironment; Tregs, regulatory T cells; TAM, tumor associated macrophages; TCGA, the cancer genome atlas; IHC, Immunohistochemistry; FCM, flow cytometry; NGS, next-gene sequencing; GO, gene ontology; KEGG, Kyoto encyclopedia of genes and genomes; BP, biological process; MF, molecular function; CC, cell composition.

Address correspondence to: Hao Zeng, Department of Urology, West China Hospital, Sichuan University, Chengdu 610041, P. R. China; Institute of Urology, West China Hospital, Sichuan University, Chengdu 610041, P. R. China. Tel: +86-18980602129; Fax: +86-18980601642; E-mail: Kucaizeng@163.com; Qiao Zhou, Department of Pathology, West China Hospital, Sichuan University, No. 37 Guoxue Xiang, Chengdu 610041, Sichuan, China; Institute of Pathology, West China Hospital, Sichuan University, No. 37 Guoxue Xiang, Chengdu 610041, Sichuan, China. Tel: +86-18980602129; Fax: +86-189-80601642; E-mail: zhou_qiao@hotmail.com

References

[1] Rini BI, Campbell SC and Escudier B. Renal cell carcinoma. Lancet 2009; 373: 1119-1132.

[2] Thompson RH, Dong H, Lohse CM, Leibovich BC, Blute ML, Cheville JC and Kwon ED. PD-1 is expressed by tumor-infiltrating immune cells and is associated with poor outcome for patients with renal cell carcinoma. Clin Cancer Res 2007; 13: 1757-1761.

[3] Janiszewska AD, Poletajew S and Wasiutynski A. Spontaneous regression of renal cell carcinoma. Contemp Oncol (Pozn) 2013; 17: 123-127.

[4] Atkins MB, Regan M and McDermott D. Update on the role of interleukin 2 and other cytokines in the treatment of patients with stage IV renal carcinoma. Clin Cancer Res 2004; 10: 6342s-6346s.

[5] Inman BA, Harrison MR and George DJ. Novel immunotherapeutic strategies in development for renal cell carcinoma. Eur Urol 2013; 63: 881-889.

[6] Herbst RS, Soria JC, Kowanetz M, Fine GD, Hamid O, Gordon MS, Sosman JA, McDermott DF, Powderly JD, Gettinger SN, Kohrt HE, Horn L, Lawrence DP, Rost S, Leabman M, Xiao Y, Mokatrin A, Koeppen H, Hegde PS, Mellman I, Chen DS and Hodi FS. Predictive correlates of response to the anti-PD-L1 antibody MPDL3280A in cancer patients. Nature 2014; 515: 563-567.

[7] Motzer RJ, Tannir NM, McDermott DF, Aren Frontera O, Melichar B, Choueiri TK, Plimack ER, Barthelemy P, Porta C, George S, Powles T, Donskov F, Neiman V, Kollmannsberger CK, Salman P, Gurney H, Hawkins R, Ravaud A, Grimm MO, Bracarda S, Barrios CH, Tomita Y, Castellano D, Rini BI, Chen AC, Mekan S, McHenry MB, Wind-Rotolo M, Doan J, Sharma P, Hammers HJ and Escudier B. Nivolumab plus Ipilimumab versus sunitinib in advanced renal-cell carcinoma. N Engl J Med 2018; 378: 1277-1290.

[8] Motzer RJ, Escudier B, McDermott DF, George S, Hammers HJ, Srinivas S, Tykodi SS, Sosman JA, Procopio G, Plimack ER, Castellano D, Choueiri TK, Gurney H, Donskov F, Bono P, Wagstaff J, Gauler TC, Ueda T, Tomita Y, Schutz FA, Kollmannsberger C, Larkin J, Ravaud A, Simon JS, Xu LA, Waxman IM and Sharma P. Nivolumab versus everolimus in advanced renal-cell carcinoma. N Engl J Med 2015; 373: 1803-1813.

[9] Motzer RJ, Penkov K, Haanen J, Rini B, Albiges L, Campbell MT, Venugopal B, Kollmannsberger C, Negrier S, Uemura M, Lee JL, Vasiliev A, Miller WH Jr, Gurney H, Schmidinger M, Larkin J, Atkins MB, Bedke J, Alekseev B, Wang J, Mariani M, Robbins PB, Chudnovsky A, Fowst C, Hariharan S, Huang B, di Pietro A and Choueiri TK. Avelumab plus Axitinib versus Sunitinib for advanced renal-cell carcinoma. N Engl J Med 2019; 380: 1103-1115.

[10] Rini BI, Plimack ER, Stus V, Gafanov R, Hawkins R, Nosov D, Pouliot F, Alekseev B, Soulieres D, Melichar B, Vynnychenko I, Kryzhanivska A, Bondarenko I, Azevedo SJ, Borchiellini D, Szczylik C, Markus M, McDermott RS, Bedke J, Tartas S, Chang YH, Tamada S, Shou Q, Perini RF, Chen M, Atkins MB and Powles T. Pembrolizumab plus axitinib versus sunitinib for advanced renal-cell carcinoma. N Engl J Med 2019; 380: 1116-1127.

[11] David FM, Lee JL, Szczylik C, Donskov F, Malik J, Alekseev BY, James MG, Larkin, Matveev VB, Gafanov RA, Tomczak P, Scott ST, Poul FG, Pawel JW, Shin SJ, Pouliot F, Gordoa TA, Li W, Rodolfo FP, Schloss C, Michael BA and Deaconess BI. Pembrolizumab monotherapy as first-line therapy in advanced clear cell renal cell carcinoma (accRCC): results from cohort A

of KEYNOTE-427. J Clin Oncol 2018; 36: abstr 4500.

[12] Robert JM, Powles T, Michael BA, Escudier B, David FM, Suarez C, Bracarda S, Stadler WM, Donskov F, Lee JL, Robert EH, Ravaud A, Boris YA, Michael DS, Uemura M, Donaldson F, Li S, Mahrukh AH, Schiff C and Brian IR. IMmotion151: arandomized phase III study of atezolizumab plus Bevacizumab vs Sunitinib in untreated metastatic renal cell carcinoma (mRCC). J Clin Oncol 2018; 36: abstr 578.

[13] Motzer RJ, Rini BI, McDermott DF, Redman BG, Kuzel TM, Harrison MR, Vaishampayan UN, Drabkin HA, George S, Logan TF, Margolin KA, Plimack ER, Lambert AM, Waxman IM and Hammers HJ. Nivolumab for metastatic renal cell carcinoma: results of a randomized phase II trial. J Clin Oncol 2015; 33: 1430-1437.

[14] Lawrence MS, Stojanov P, Polak P, Kryukov GV, Cibulskis K, Sivachenko A, Carter SL, Stewart C, Mermel CH, Roberts SA, Kiezun A, Hammerman PS, McKenna A, Drier Y, Zou L, Ramos AH, Pugh TJ, Stransky N, Helman E, Kim J, Sougnez C, Ambrogio L, Nickerson E, Shefler E, Cortes ML, Auclair D, Saksena G, Voet D, Noble M, DiCara D, Lin P, Lichtenstein L, Heiman DI, Fennell T, Imielinski M, Hernandez B, Hodis E, Baca S, Dulak AM, Lohr J, Landau DA, Wu CJ, Melendez-Zajgla J, Hidalgo-Miranda A, Koren A, McCarroll SA, Mora J, Crompton B, Onofrio R, Parkin M, Winckler W, Ardlie K, Gabriel SB, Roberts CWM, Biegel JA, Stegmaier K, Bass AJ, Garraway LA, Meyerson M, Golub TR, Gordenin DA, Sunyaev S, Lander ES and Getz G. Mutational heterogeneity in cancer and the search for new cancer-associated genes. Nature 2013; 499: 214-218.

[15] Carbognin L, Pilotto S, Milella M, Vaccaro V, Brunelli M, Calio A, Cuppone F, Sperduti I, Giannarelli D, Chilosi M, Bronte V, Scarpa A, Bria E and Tortora G. Differential activity of nivolumab, pembrolizumab and MPDL3280A according to the tumor expression of programmed death-ligand-1 (PD-L1): sensitivity analysis of trials in melanoma, lung and genitourinary cancers. PLoS One 2015; 10: e0130142.

[16] Correa AF, Jegede O, Haas NB, Flaherty KT, Pins MR, Messing EM, Manola J, Wood CG, Kane CJ, Jewett MAS, Dutcher JP, DiPaola RS, Carducci MA and Uzzo RG. Predicting renal cancer recurrence: defining limitations of existing prognostic models with prospective trial-based validation. J Clin Oncol 2019; 37: 2062-2071.

[17] Turajlic S, Litchfield K, Xu H, Rosenthal R, McGranahan N, Reading JL, Wong YNS, Rowan A, Kanu N, Al Bakir M, Chambers T, Salgado R, Savas P, Loi S, Birkbak NJ, Sansregret L, Gore M, Larkin J, Quezada SA and Swanton C. Insertion-and-deletion-derived tumour-specific neoantigens and the immunogenic phenotype: a pan-cancer analysis. Lancet Oncol 2017; 18: 1009-1021.

[18] McDermott DF, Huseni MA, Atkins MB, Motzer RJ, Rini BI, Escudier B, Fong L, Joseph RW, Pal SK, Reeves JA, Sznol M, Hainsworth J, Rathmell WK, Stadler WM, Hutson T, Gore ME, Ravaud A, Bracarda S, Suarez C, Danielli R, Gruenwald V, Choueiri TK, Nickles D, Jhunjhunwala S, Piault-Louis E, Thobhani A, Qiu J, Chen DS, Hegde PS, Schiff C, Fine GD and Powles T. Clinical activity and molecular correlates of response to atezolizumab alone or in combination with bevacizumab versus sunitinib in renal cell carcinoma. Nat Med 2018; 24: 749-757.

[19] Rooney MS, Shukla SA, Wu CJ, Getz G and Hacohen N. Molecular and genetic properties of tumors associated with local immune cytolytic activity. Cell 2015; 160: 48-61.

[20] Pitt JM, Marabelle A, Eggermont A, Soria JC, Kroemer G and Zitvogel L. Targeting the tumor microenvironment: removing obstruction to anticancer immune responses and immunotherapy. Ann Oncol 2016; 27: 1482-1492.

[21] Hinshaw DC and Shevde LA. The tumor microenvironment innately modulates cancer progression. Cancer Res 2019; 79: 4557-4566.

[22] Hanahan D and Coussens LM. Accessories to the crime: functions of cells recruited to the tumor microenvironment. Cancer Cell 2012; 21: 309-322.

[23] Nishikawa H and Sakaguchi S. Regulatory T cells in cancer immunotherapy. Curr Opin Immunol 2014; 27: 1-7.

[24] Noy R and Pollard JW. Tumor-associated macrophages: from mechanisms to therapy. Immunity 2014; 41: 49-61.

[25] Gajewski TF, Schreiber H and Fu YX. Innate and adaptive immune cells in the tumor microenvironment. Nat Immunol 2013; 14: 1014-1022.

[26] Galon J, Costes A, Sanchez-Cabo F, Kirilovsky A, Mlecnik B, Lagorce-Pages C, Tosolini M, Camus M, Berger A, Wind P, Zinzindohoue F, Bruneval P, Cugnenc PH, Trajanoski Z, Fridman WH and Pages F. Type, density, and location of immune cells within human colorectal tumors predict clinical outcome. Science 2006; 313: 1960-1964.

[27] Pages F, Kirilovsky A, Mlecnik B, Asslaber M, Tosolini M, Bindea G, Lagorce C, Wind P, Marliot F, Bruneval P, Zatloukal K, Trajanoski Z, Berger A, Fridman WH and Galon J. In situ cytotoxic and memory T cells predict outcome in patients with early-stage colorectal cancer. J Clin Oncol 2009; 27: 5944-5951.

[28] Choueiri TK, Fishman MN, Escudier B, McDermott DF, Drake CG, Kluger H, Stadler WM, Perez-Gracia JL, McNeel DG, Curti B, Harrison MR,

Plimack ER, Appleman L, Fong L, Albiges L, Cohen L, Young TC, Chasalow SD, Ross-Macdonald P, Srivastava S, Jure-Kunkel M, Kurland JF, Simon JS and Sznol M. Immunomodulatory activity of nivolumab in metastatic renal cell carcinoma. Clin Cancer Res 2016; 22: 5461-5471.

[29] Senbabaoglu Y, Gejman RS, Winer AG, Liu M, Van Allen EM, de Velasco G, Miao D, Ostrovnaya I, Drill E, Luna A, Weinhold N, Lee W, Manley BJ, Khalil DN, Kaffenberger SD, Chen Y, Danilova L, Voss MH, Coleman JA, Russo P, Reuter VE, Chan TA, Cheng EH, Scheinberg DA, Li MO, Choueiri TK, Hsieh JJ, Sander C and Hakimi AA. Tumor immune microenvironment characterization in clear cell renal cell carcinoma identifies prognostic and immunotherapeutically relevant messenger RNA signatures. Genome Biol 2016; 17: 231.

[30] Chen YP, Zhang Y, Lv JW, Li YQ, Wang YQ, He QM, Yang XJ, Sun Y, Mao YP, Yun JP, Liu N and Ma J. Genomic analysis of tumor microenvironment immune types across 14 solid cancer types: immunotherapeutic implications. Theranostics 2017; 7: 3585-3594.

[31] Carter SL, Cibulskis K, Helman E, McKenna A, Shen H, Zack T, Laird PW, Onofrio RC, Winckler W, Weir BA, Beroukhim R, Pellman D, Levine DA, Lander ES, Meyerson M and Getz G. Absolute quantification of somatic DNA alterations in human cancer. Nat Biotechnol 2012; 30: 413-421.

[32] Yoshihara K, Shahmoradgoli M, Martinez E, Vegesna R, Kim H, Torres-Garcia W, Trevino V, Shen H, Laird PW, Levine DA, Carter SL, Getz G, Stemke-Hale K, Mills GB and Verhaak RG. Inferring tumour purity and stromal and immune cell admixture from expression data. Nat Commun 2013; 4: 2612.

[33] Song E, Song W, Ren M, Xing L, Ni W, Li Y, Gong M, Zhao M, Ma X, Zhang X and An R. Identification of potential crucial genes associated with carcinogenesis of clear cell renal cell carcinoma. J Cell Biochem 2018; 119: 5163-5174.

[34] Linehan WM and Ricketts CJ. The Cancer Genome Atlas of renal cell carcinoma: findings and clinical implications. Nat Rev Urol 2019; 16: 539-552.

[35] Ritchie ME, Phipson B, Wu D, Hu Y, Law CW, Shi W and Smyth GK. limma powers differential expression analyses for RNA-sequencing and microarray studies. Nucleic Acids Res 2015; 43: e47.

[36] Huang da W, Sherman BT and Lempicki RA. Systematic and integrative analysis of large gene lists using DAVID bioinformatics resources. Nat Protoc 2009; 4: 44-57.

[37] Szklarczyk D, Franceschini A, Wyder S, Forslund K, Heller D, Huerta-Cepas J, Simonovic M, Roth A, Santos A, Tsafou KP, Kuhn M, Bork P, Jensen LJ and von Mering C. STRING v10: protein-protein interaction networks, integrated over the tree of life. Nucleic Acids Res 2015; 43: D447-452.

[38] Shannon P, Markiel A, Ozier O, Baliga NS, Wang JT, Ramage D, Amin N, Schwikowski B and Ideker T. Cytoscape: a software environment for integrated models of biomolecular interaction networks. Genome Res 2003; 13: 2498-2504.

[39] Newman AM, Liu CL and Green MR. Robust enumeration of cell subsets from tissue expression profiles. Nat Methods 2015; 12: 453-457.

[40] Sharma P and Allison JP. The future of immune checkpoint therapy. Science 2015; 348: 56-61.

[41] Atkins MB, Clark JI and Quinn DI. Immune checkpoint inhibitors in advanced renal cell carcinoma: experience to date and future directions. Ann Oncol 2017; 28: 1484-1494.

[42] Hutchins AP, Diez D and Miranda-Saavedra D. The IL-10/STAT3-mediated anti-inflammatory response: recent developments and future challenges. Brief Funct Genomics 2013; 12: 489-498.

[43] Shouval DS, Ouahed J, Biswas A, Goettel JA, Horwitz BH, Klein C, Muise AM and Snapper SB. Interleukin 10 receptor signaling: master regulator of intestinal mucosal homeostasis in mice and humans. Adv Immunol 2014; 122: 177-210.

[44] Tsuji M, Ezumi Y, Arai M and Takayama H. A novel association of Fc receptor gamma-chain with glycoprotein VI and their co-expression as a collagen receptor in human platelets. J Biol Chem 1997; 272: 23528-23531.

[45] Andreu P, Johansson M, Affara NI, Pucci F, Tan T, Junankar S, Korets L, Lam J, Tawfik D, DeNardo DG, Naldini L, de Visser KE, De Palma M and Coussens LM. FcRgamma activation regulates inflammation-associated squamous carcinogenesis. Cancer Cell 2010; 17: 121-134.

[46] Chen L, Yuan L, Wang Y, Wang G, Zhu Y, Cao R, Qian G, Xie C, Liu X, Xiao Y and Wang X. Co-expression network analysis identified FCER1G in association with progression and prognosis in human clear cell renal cell carcinoma. Int J Biol Sci 2017; 13: 1361-1372.

[47] Li L, Peng M, Xue W, Fan Z, Wang T, Lian J, Zhai Y, Lian W, Qin D and Zhao J. Integrated analysis of dysregulated long non-coding RNAs/microRNAs/mRNAs in metastasis of lung adenocarcinoma. J Transl Med 2018; 16: 372.

[48] Schieffer KM, Choi CS, Emrich S, Harris L, Deiling S, Karamchandani DM, Salzberg A, Kawasawa YI, Yochum GS and Koltun WA. RNA-seq implicates deregulation of the immune system

in the pathogenesis of diverticulitis. Am J Physiol Gastrointest Liver Physiol 2017; 313: G277-G284.

[49] Sanati N, Iancu OD, Wu G, Jacobs JE and McWeeney SK. Network-based predictors of progression in head and neck squamous cell carcinoma. Front Genet 2018; 9: 183.

[50] Erdem-Eraslan L, Heijsman D, de Wit M, Kremer A, Sacchetti A, van der Spek PJ, Sillevis Smitt PA and French PJ. Tumor-specific mutations in low-frequency genes affect their functional properties. J Neurooncol 2015; 122: 461-470.

[51] Troeger A and Williams DA. Hematopoietic-specific Rho GTPases Rac2 and RhoH and human blood disorders. Exp Cell Res 2013; 319: 2375-2383.

[52] Voena C and Chiarle R. RHO family GTPases in the biology of lymphoma. Cells 2019; 8: 646.

[53] Woldu SL, Hutchinson RC, Krabbe LM, Sanli O and Margulis V. The Rho GTPase signalling pathway in urothelial carcinoma. Nat Rev Urol 2018; 15: 83-91.

[54] Chen L, Wang G, Luo Y, Wang Y, Xie C, Jiang W, Xiao Y, Qian G and Wang X. Downregulation of LAPTM5 suppresses cell proliferation and viability inducing cell cycle arrest at G0/G1 phase of bladder cancer cells. Int J Oncol 2017; 50: 263-271.

[55] Dierks S, von Hardenberg S, Schmidt T, Bremmer F, Burfeind P and Kaulfuss S. Leupaxin stimulates adhesion and migration of prostate cancer cells through modulation of the phosphorylation status of the actin-binding protein caldesmon. Oncotarget 2015; 6: 13591-13606.

[56] Hou T, Zhou L, Wang L, Kazobinka G, Chen Y, Zhang X and Chen Z. Leupaxin promotes bladder cancer proliferation, metastasis, and angiogenesis through the PI3K/AKT pathway. Cell Physiol Biochem 2018; 47: 2250-2260.

[57] Zhang X, Zhang H, Chen L, Feng Z, Gao L and Li Q. TIGIT expression is upregulated in T cells and causes T cell dysfunction independent of PD-1 and Tim-3 in adult B lineage acute lymphoblastic leukemia. Cell Immunol 2019; 344: 103958.

[58] Liu XG, Hou M and Liu Y. TIGIT, a novel therapeutic target for tumor immunotherapy. Immunol Invest 2017; 46: 172-182.

[59] Robinson RT. IL12Rbeta1: the cytokine receptor that we used to know. Cytokine 2015; 71: 348-359.

[60] Zhao YY, Yan DJ and Chen ZW. Role of AIF-1 in the regulation of inflammatory activation and diverse disease processes. Cell Immunol 2013; 284: 75-83.

[61] Karaky M, Fedetz M, Potenciano V, Andres-Leon E, Codina AE, Barrionuevo C, Alcina A and Matesanz F. SP140 regulates the expression of immune-related genes associated with multiple sclerosis and other autoimmune diseases by NF-kappaB inhibition. Hum Mol Genet 2018; 27: 4012-4023.

[62] Nakano O, Sato M, Naito Y, Suzuki K, Orikasa S, Aizawa M, Suzuki Y, Shintaku I, Nagura H and Ohtani H. Proliferative activity of intratumoral CD8(+) T-lymphocytes as a prognostic factor in human renal cell carcinoma: clinicopathologic demonstration of antitumor immunity. Cancer Res 2001; 61: 5132-5136.

[63] Mella M, Kauppila JH, Karihtala P, Lehenkari P, Jukkola-Vuorinen A, Soini Y, Auvinen P, Vaarala MH, Ronkainen H, Kauppila S, Haapasaari KM, Vuopala KS and Selander KS. Tumor infiltrating CD8(+) T lymphocyte count is independent of tumor TLR9 status in treatment naive triple negative breast cancer and renal cell carcinoma. Oncoimmunology 2015; 4: e1002726.

[64] Bromwich EJ, McArdle PA, Canna K, McMillan DC, McNicol AM, Brown M and Aitchison M. The relationship between T-lymphocyte infiltration, stage, tumour grade and survival in patients undergoing curative surgery for renal cell cancer. Br J Cancer 2003; 89: 1906-1908.

[65] Hotta K, Sho M, Fujimoto K, Shimada K, Yamato I, Anai S, Konishi N, Hirao Y, Nonomura K and Nakajima Y. Prognostic significance of CD45RO+ memory T cells in renal cell carcinoma. Br J Cancer 2011; 105: 1191-1196.

[66] Chevrier S, Levine JH, Zanotelli VRT, Silina K, Schulz D, Bacac M, Ries CH, Ailles L, Jewett MAS, Moch H, van den Broek M, Beisel C, Stadler MB, Gedye C, Reis B, Pe'er D and Bodenmiller B. An immune atlas of clear cell renal cell carcinoma. Cell 2017; 169: 736-749, e718.

[67] Pages F, Mlecnik B, Marliot F, Bindea G, Ou FS, Bifulco C, Lugli A, Zlobec I, Rau TT, Berger MD, Nagtegaal ID, Vink-Borger E, Hartmann A, Geppert C, Kolwelter J, Merkel S, Grutzmann R, Van den Eynde M, Jouret-Mourin A, Kartheuser A, Leonard D, Remue C, Wang JY, Bavi P, Roehrl MHA, Ohashi PS, Nguyen LT, Han S, MacGregor HL, Hafezi-Bakhtiari S, Wouters BG, Masucci GV, Andersson EK, Zavadova E, Vocka M, Spacek J, Petruzelka L, Konopasek B, Dundr P, Skalova H, Nemejcova K, Botti G, Tatangelo F, Delrio P, Ciliberto G, Maio M, Laghi L, Grizzi F, Fredriksen T, Buttard B, Angelova M, Vasaturo A, Maby P, Church SE, Angell HK, Lafontaine L, Bruni D, El Sissy C, Haicheur N, Kirilovsky A, Berger A, Lagorce C, Meyers JP, Paustian C, Feng Z, Ballesteros-Merino C, Dijkstra J, van de Water C, van Lent-van Vliet S, Knijn N, Musina AM, Scripcariu DV, Popivanova B, Xu M, Fujita T, Hazama S, Suzuki N, Nagano H, Okuno K, Torigoe T, Sato N, Furuhata T,

Takemasa I, Itoh K, Patel PS, Vora HH, Shah B, Patel JB, Rajvik KN, Pandya SJ, Shukla SN, Wang Y, Zhang G, Kawakami Y, Marincola FM, Ascierto PA, Sargent DJ, Fox BA and Galon J. International validation of the consensus immunoscore for the classification of colon cancer: a prognostic and accuracy study. Lancet 2018; 391: 2128-2139.

[68] Kawakami F, Sircar K, Rodriguez-Canales J, Fellman BM, Urbauer DL, Tamboli P, Tannir NM, Jonasch E, Wistuba II, Wood CG and Karam JA. Programmed cell death ligand 1 and tumor-infiltrating lymphocyte status in patients with renal cell carcinoma and sarcomatoid dedifferentiation. Cancer 2017; 123: 4823-4831.

[69] Xu WH, Xu Y, Wang J, Wan FN, Wang HK, Cao DL, Shi GH, Qu YY, Zhang HL and Ye DW. Prognostic value and immune infiltration of novel signatures in clear cell renal cell carcinoma microenvironment. Aging (Albany NY) 2019; 11: 6999-7020.

Table S1. The relationships of the 1433 up-regulated genes to OS

Genes	HR [exp (coef)]	coef	95% CI lower	95% CI upper	Z	*P* value
ADAMTS14	1.42	0.351	0.271	0.431	8.554	0
KIF18B	1.578	0.456	0.349	0.563	8.372	0
UBE2C	1.489	0.398	0.306	0.49	8.472	0
AURKB	1.583	0.459	0.351	0.567	8.343	0
FAM72B	1.976	0.681	0.53	0.833	8.804	0
HJURP	1.628	0.487	0.369	0.606	8.062	0
LRP8	1.714	0.539	0.407	0.67	8.034	0
ADAM8	1.561	0.445	0.336	0.555	7.989	0
CENPA	1.607	0.474	0.357	0.591	7.947	0
NUF2	1.657	0.505	0.379	0.631	7.841	0
BIRC5	1.501	0.406	0.304	0.508	7.837	0
FKBP11	1.7	0.531	0.396	0.666	7.689	0
TNNT1	1.195	0.179	0.133	0.224	7.623	0
PTTG1	1.584	0.46	0.341	0.579	7.583	0
OTOF	1.525	0.422	0.313	0.532	7.553	0
TACC3	2.036	0.711	0.526	0.896	7.53	0
PIF1	1.505	0.409	0.301	0.516	7.466	0
KCNN4	1.51	0.412	0.304	0.52	7.447	0
IGF2BP3	1.269	0.238	0.176	0.301	7.438	0
KIF2C	1.625	0.486	0.357	0.614	7.4	0
PTPRH	1.198	0.181	0.133	0.229	7.362	0
CEP55	1.61	0.476	0.348	0.604	7.312	0
RELT	2.091	0.738	0.538	0.937	7.253	0
HN1	1.827	0.603	0.439	0.766	7.225	0
MYBL2	1.437	0.362	0.264	0.461	7.187	0
MX2	1.843	0.612	0.444	0.779	7.169	0
PLAUR	1.603	0.472	0.343	0.601	7.154	0
PPP2R2C	1.23	0.207	0.15	0.263	7.149	0
NEIL3	1.5	0.405	0.293	0.517	7.092	0
DLX4	1.414	0.346	0.25	0.443	7.041	0
SLC17A9	1.374	0.318	0.229	0.407	7.024	0
RGS20	1.322	0.279	0.201	0.357	6.99	0
ITIH4	1.227	0.204	0.147	0.261	6.986	0
LIMK1	1.81	0.593	0.427	0.76	6.986	0
TFAP2E	1.741	0.554	0.399	0.71	6.98	0
SPOCD1	1.357	0.305	0.219	0.391	6.946	0
NCAPG	1.714	0.539	0.385	0.692	6.888	0
RUFY4	1.323	0.28	0.2	0.36	6.858	0
WNT10B	1.401	0.337	0.241	0.434	6.833	0
MFI2	1.258	0.23	0.164	0.296	6.817	0
GFPT2	1.282	0.248	0.177	0.32	6.81	0
ANXA8	1.221	0.2	0.142	0.258	6.772	0
KIF14	1.54	0.432	0.307	0.557	6.767	0
SLC38A5	1.199	0.181	0.129	0.234	6.739	0
SAA1	1.122	0.115	0.082	0.149	6.732	0
CPNE7	1.284	0.25	0.177	0.323	6.714	0
CDCA7	1.496	0.403	0.285	0.521	6.708	0

FAM54A	1.713	0.539	0.381	0.696	6.689	0
SH3BGRL3	1.709	0.536	0.379	0.693	6.679	0
C9orf109	1.541	0.432	0.305	0.559	6.679	0
NIPAL4	1.249	0.223	0.157	0.288	6.664	0
PAEP	1.135	0.127	0.089	0.164	6.661	0
GRIN2D	1.454	0.374	0.264	0.485	6.645	0
IL20RB	1.176	0.162	0.114	0.21	6.644	0
COL22A1	1.229	0.206	0.145	0.267	6.633	0
PITX1	1.188	0.173	0.121	0.224	6.609	0
FLJ40330	1.284	0.25	0.176	0.324	6.596	0
ARHGAP4	1.723	0.544	0.381	0.707	6.55	0
SPHK1	1.436	0.362	0.252	0.472	6.431	0
STEAP3	1.303	0.265	0.184	0.345	6.427	0
MIAT	1.305	0.266	0.185	0.347	6.413	0
JAK3	1.536	0.429	0.297	0.562	6.355	0
HAPLN3	1.534	0.428	0.296	0.56	6.349	0
PLA2G2A	1.176	0.162	0.112	0.212	6.348	0
MDK	1.346	0.297	0.206	0.389	6.343	0
GSG2	1.671	0.514	0.354	0.673	6.32	0
IKBKE	1.606	0.474	0.326	0.621	6.304	0
GPR84	1.449	0.371	0.255	0.486	6.288	0
PLTP	1.313	0.272	0.187	0.358	6.258	0
BASP1	1.412	0.345	0.237	0.453	6.257	0
NCAPH	1.584	0.46	0.315	0.605	6.232	0
ASGR1	1.355	0.304	0.208	0.4	6.231	0
UNC13D	1.619	0.482	0.329	0.634	6.193	0
SRPX2	1.236	0.212	0.144	0.279	6.181	0
SLC11A1	1.47	0.386	0.263	0.508	6.172	0
FAM20A	1.379	0.322	0.219	0.424	6.166	0
PI3	1.17	0.157	0.107	0.207	6.162	0
SAA2	1.118	0.112	0.076	0.147	6.141	0
DOK3	1.67	0.513	0.349	0.676	6.134	0
KIAA1949	2.193	0.785	0.534	1.036	6.131	0
SERPINF1	1.316	0.275	0.187	0.362	6.126	0
UHRF1	1.533	0.427	0.29	0.564	6.112	0
STYK1	1.429	0.357	0.242	0.471	6.109	0
TNFSF14	1.316	0.275	0.187	0.363	6.108	0
FZD2	1.442	0.366	0.248	0.484	6.076	0
LAT	1.416	0.348	0.235	0.46	6.07	0
MOCOS	1.236	0.212	0.143	0.28	6.048	0
RNF175	1.356	0.304	0.206	0.403	6.045	0
KIAA1324	1.284	0.25	0.169	0.331	6.043	0
RRM2	1.49	0.399	0.269	0.528	6.023	0
CENPE	1.482	0.393	0.265	0.522	6.006	0
LOC389634	1.405	0.34	0.229	0.451	6.006	0
C10orf81	1.196	0.179	0.12	0.237	5.99	0
HAMP	1.262	0.233	0.156	0.309	5.937	0
EREG	1.234	0.21	0.141	0.28	5.917	0
PLEKHO1	1.677	0.517	0.346	0.688	5.914	0

RUNX1	1.579	0.457	0.305	0.609	5.898	0
BUB1	1.433	0.36	0.24	0.48	5.893	0
RRN3P2	1.441	0.365	0.244	0.487	5.89	0
HSH2D	1.387	0.327	0.218	0.436	5.882	0
CMTM7	1.801	0.588	0.391	0.785	5.86	0
MAT1A	1.156	0.145	0.097	0.194	5.859	0
IL6	1.173	0.159	0.106	0.213	5.848	0
ZNF385A	1.589	0.463	0.308	0.619	5.831	0
SEMA7A	1.524	0.421	0.279	0.564	5.804	0
LMNB1	1.775	0.574	0.379	0.769	5.783	0
TRAF5	1.672	0.514	0.34	0.688	5.776	0
RYR2	1.199	0.181	0.12	0.243	5.771	0
C1R	1.34	0.293	0.193	0.392	5.769	0
ERMN	1.403	0.339	0.223	0.454	5.752	0
CLEC2B	1.534	0.428	0.282	0.573	5.751	0
MUC12	1.244	0.219	0.144	0.293	5.747	0
SOCS1	1.377	0.32	0.211	0.429	5.744	0
CARD14	1.258	0.23	0.151	0.308	5.74	0
HK3	1.473	0.388	0.255	0.52	5.718	0
S1PR2	1.585	0.46	0.303	0.618	5.717	0
TNFRSF18	1.364	0.31	0.203	0.417	5.7	0
OSCAR	1.541	0.432	0.283	0.582	5.678	0
AIM2	1.291	0.255	0.167	0.343	5.664	0
MRC2	1.425	0.354	0.231	0.477	5.646	0
NTNG2	1.321	0.279	0.182	0.376	5.646	0
HS3ST3A1	1.27	0.239	0.156	0.323	5.642	0
POLQ	1.464	0.381	0.249	0.514	5.639	0
C1orf96	1.72	0.543	0.354	0.731	5.638	0
BLM	1.617	0.48	0.313	0.648	5.624	0
CD44	1.47	0.385	0.251	0.52	5.609	0
IL27	1.471	0.386	0.251	0.521	5.608	0
RNASE2	1.37	0.315	0.205	0.425	5.596	0
PMAIP1	1.387	0.327	0.212	0.442	5.595	0
ASPM	1.426	0.355	0.23	0.479	5.592	0
MAP3K8	1.626	0.486	0.315	0.657	5.579	0
ARPC1B	1.773	0.573	0.371	0.774	5.578	0
ANXA8L2	1.188	0.172	0.112	0.232	5.575	0
APCDD1L	1.183	0.168	0.109	0.227	5.571	0
UGT1A10	1.131	0.123	0.08	0.166	5.558	0
FAM101A	1.179	0.164	0.106	0.222	5.548	0
HSPA7	1.293	0.257	0.166	0.348	5.543	0
ARSI	1.218	0.197	0.127	0.267	5.531	0
SAA4	1.159	0.147	0.095	0.199	5.53	0
MFSD2A	1.215	0.194	0.125	0.264	5.518	0
AIM1L	1.269	0.238	0.154	0.323	5.515	0
FAM78B	1.41	0.344	0.222	0.466	5.512	0
CHI3L2	1.222	0.201	0.129	0.272	5.503	0
TM4SF19	1.233	0.209	0.135	0.284	5.498	0
ARHGAP22	1.674	0.515	0.331	0.699	5.493	0
C1S	1.308	0.269	0.173	0.364	5.492	0

EPHB2	1.385	0.325	0.209	0.442	5.488	0
JSRP1	1.205	0.187	0.12	0.253	5.482	0
IL15RA	1.701	0.531	0.341	0.722	5.475	0
STAC3	1.613	0.478	0.307	0.649	5.474	0
IL23A	1.587	0.462	0.296	0.628	5.451	0
XAF1	1.479	0.391	0.25	0.532	5.427	0
KIF15	1.41	0.343	0.219	0.467	5.423	0
LIMD2	1.48	0.392	0.25	0.534	5.418	0
VNN3	1.299	0.262	0.167	0.357	5.4	0
ZNF365	1.22	0.199	0.127	0.271	5.4	0
SP5	1.196	0.179	0.114	0.244	5.39	0
SLPI	1.12	0.113	0.072	0.155	5.384	0
COL11A1	1.151	0.14	0.089	0.192	5.379	0
C17orf66	1.444	0.368	0.234	0.502	5.379	0
ABCA7	1.456	0.376	0.239	0.513	5.377	0
APOL2	1.505	0.408	0.259	0.558	5.362	0
PLAU	1.385	0.326	0.207	0.445	5.36	0
FAM179A	1.371	0.315	0.2	0.431	5.348	0
KLRC2	1.372	0.316	0.2	0.432	5.347	0
C4orf7	1.142	0.133	0.084	0.181	5.346	0
ENTHD1	1.381	0.323	0.204	0.441	5.331	0
TRIM36	1.462	0.38	0.239	0.52	5.31	0
LBP	1.096	0.092	0.058	0.126	5.308	0
NOD2	1.398	0.335	0.211	0.459	5.307	0
SLN	1.153	0.143	0.09	0.195	5.303	0
RUNX2	1.51	0.412	0.26	0.565	5.297	0
PPP1R1A	1.115	0.108	0.068	0.149	5.287	0
FANCA	1.42	0.351	0.22	0.482	5.259	0
INSL3	1.346	0.297	0.186	0.408	5.253	0
SEMA3A	1.259	0.231	0.145	0.317	5.253	0
NCF4	1.542	0.433	0.271	0.595	5.242	0
PBX4	1.356	0.305	0.191	0.418	5.237	0
DERL3	1.291	0.256	0.16	0.352	5.236	0
CXCL1	1.181	0.167	0.104	0.229	5.233	0
IFI16	1.866	0.624	0.39	0.858	5.23	0
NFE2L3	1.529	0.425	0.265	0.584	5.225	0
FXYD5	1.623	0.484	0.302	0.666	5.221	0
ADAM12	1.218	0.197	0.123	0.271	5.217	0
CPA4	1.139	0.13	0.081	0.179	5.212	0
DLGAP5	1.4	0.336	0.21	0.463	5.198	0
TXNDC3	1.452	0.373	0.232	0.513	5.19	0
C11orf45	1.426	0.355	0.221	0.489	5.182	0
ADA	1.367	0.313	0.195	0.431	5.18	0
SALL4	1.242	0.217	0.135	0.299	5.175	0
TMEM149	1.504	0.408	0.253	0.563	5.166	0
FCGR1C	1.403	0.339	0.21	0.468	5.144	0
RHEBL1	1.578	0.456	0.282	0.63	5.138	0
PYCARD	1.421	0.352	0.217	0.486	5.125	0
BEND6	1.27	0.239	0.147	0.33	5.125	0
HP	1.094	0.09	0.055	0.124	5.118	0

HSPA6	1.323	0.28	0.172	0.387	5.11	0
MMP12	1.158	0.146	0.09	0.202	5.108	0
EPYC	1.272	0.241	0.148	0.333	5.106	0
ISG20	1.481	0.393	0.241	0.544	5.071	0
CATSPER1	1.347	0.298	0.183	0.413	5.064	0
SGOL1	1.411	0.344	0.211	0.477	5.055	0
C4orf48	1.223	0.201	0.123	0.279	5.054	0
EFNA5	1.211	0.192	0.117	0.266	5.043	0
CCDC88B	1.409	0.343	0.21	0.476	5.042	0
MS4A14	1.351	0.301	0.184	0.418	5.037	0
FCHO1	1.297	0.26	0.159	0.362	5.029	0
CASP4	1.969	0.678	0.413	0.942	5.022	0
CXCL5	1.123	0.116	0.071	0.162	5.021	0
ADAM19	1.447	0.369	0.225	0.513	5.014	0
MIR155HG	1.282	0.248	0.151	0.345	5.013	0
CEACAM4	1.331	0.286	0.174	0.397	5.013	0
CD7	1.317	0.275	0.167	0.383	4.99	0
TNFRSF8	1.514	0.415	0.252	0.578	4.984	0
PIK3R6	1.354	0.303	0.184	0.422	4.983	0
HMGA1	1.422	0.352	0.213	0.49	4.981	0
ZNF80	1.306	0.267	0.162	0.372	4.976	0
APBA2	1.262	0.233	0.141	0.325	4.972	0
SHCBP1	1.385	0.326	0.197	0.455	4.964	0
OSM	1.279	0.246	0.149	0.343	4.955	0
POU2F2	1.358	0.306	0.185	0.428	4.935	0
ZP1	1.174	0.161	0.097	0.224	4.934	0
EFHD2	1.736	0.551	0.332	0.771	4.929	0
CXorf30	1.178	0.164	0.099	0.229	4.927	0
ATP8B3	1.212	0.192	0.116	0.269	4.92	0
RGS19	1.766	0.569	0.342	0.795	4.918	0
KLHDC7B	1.253	0.226	0.136	0.316	4.91	0
MKI67	1.424	0.353	0.212	0.495	4.903	0
ARL4C	1.345	0.296	0.178	0.415	4.9	0
OASL	1.386	0.327	0.196	0.458	4.894	0
FAM18A	1.429	0.357	0.214	0.5	4.892	0
HHLA2	0.891	-0.115	-0.161	-0.069	-4.886	0
TREM1	1.221	0.2	0.12	0.28	4.884	0
CXorf65	1.365	0.311	0.186	0.436	4.879	0
PIM2	1.363	0.31	0.185	0.435	4.873	0
GPSM3	1.589	0.463	0.277	0.65	4.866	0
GPR68	1.375	0.319	0.19	0.447	4.86	0
FCGR1B	1.383	0.324	0.193	0.455	4.858	0
F2	1.11	0.105	0.062	0.147	4.847	0
MYBL1	1.392	0.331	0.197	0.465	4.837	0
CD72	1.342	0.294	0.175	0.413	4.832	0
FOXP3	1.247	0.221	0.131	0.311	4.813	0
BATF	1.312	0.271	0.161	0.382	4.803	0
ZBP1	1.278	0.245	0.145	0.346	4.798	0
TRPM8	1.201	0.183	0.108	0.258	4.782	0
IL8	1.192	0.175	0.103	0.247	4.779	0

DEF6	1.445	0.368	0.217	0.519	4.776	0
HCST	1.385	0.325	0.192	0.459	4.775	0
WFDC5	1.139	0.13	0.076	0.183	4.774	0
PADI3	1.125	0.117	0.069	0.166	4.762	0
CYBA	1.471	0.386	0.227	0.545	4.758	0
APOBEC3D	1.489	0.398	0.234	0.563	4.74	0
LOXL3	1.341	0.294	0.172	0.415	4.738	0
CHST11	1.555	0.442	0.259	0.625	4.729	0
ASPHD2	1.323	0.28	0.164	0.396	4.727	0
PARVG	1.436	0.362	0.212	0.512	4.725	0
P2RY6	1.38	0.322	0.188	0.455	4.717	0
OBFC2A	1.541	0.432	0.252	0.613	4.705	0
CTLA4	1.256	0.228	0.133	0.323	4.704	0
DGKA	1.504	0.408	0.238	0.578	4.703	0
SH2D2A	1.279	0.246	0.143	0.349	4.691	0
LY96	1.37	0.315	0.183	0.447	4.683	0
HSD11B1	1.203	0.185	0.107	0.262	4.683	0
TRPM2	1.414	0.347	0.201	0.492	4.675	0
BTBD11	1.188	0.173	0.1	0.245	4.674	0
IL1RN	1.273	0.241	0.14	0.342	4.671	0
CCL11	1.191	0.175	0.102	0.249	4.67	0
KIAA1644	1.179	0.165	0.096	0.234	4.665	0
ICAM4	1.373	0.317	0.184	0.451	4.663	0
C5orf58	1.329	0.285	0.165	0.405	4.659	0
PRAME	1.124	0.117	0.068	0.167	4.653	0
RGS10	1.507	0.41	0.237	0.583	4.648	0
IGFBP1	1.097	0.093	0.054	0.132	4.646	0
PRDM8	1.283	0.249	0.144	0.355	4.642	0
COL10A1	1.159	0.148	0.085	0.21	4.633	0
TICAM2	1.642	0.496	0.285	0.706	4.621	0
C9orf110	1.385	0.326	0.188	0.465	4.615	0
TMC8	1.375	0.318	0.183	0.454	4.613	0
TREML1	1.389	0.328	0.189	0.468	4.607	0
TMPRSS6	1.186	0.171	0.098	0.244	4.603	0
RARRES1	1.18	0.165	0.095	0.236	4.601	0
CXCL13	1.15	0.139	0.08	0.199	4.599	0
CTHRC1	1.224	0.202	0.116	0.289	4.594	0
IL4I1	1.375	0.318	0.182	0.454	4.577	0
MMP9	1.168	0.155	0.089	0.221	4.573	0
ARHGAP9	1.37	0.315	0.18	0.45	4.566	0
FMNL1	1.499	0.405	0.231	0.579	4.564	0
GPR115	1.157	0.146	0.083	0.208	4.563	0
TNFRSF6B	1.225	0.203	0.116	0.29	4.56	0
MGC29506	1.151	0.14	0.08	0.201	4.56	0
TNFSF4	1.527	0.423	0.241	0.606	4.56	0
MYBPC2	1.197	0.18	0.103	0.257	4.559	0
KCNK17	1.168	0.155	0.089	0.222	4.555	0
RAET1K	1.454	0.374	0.213	0.536	4.546	0
LRRC15	1.147	0.137	0.078	0.196	4.533	0
MGC12916	1.44	0.365	0.207	0.523	4.532	0

CKAP2L	1.384	0.325	0.184	0.466	4.531	0
RGS2	1.314	0.273	0.155	0.391	4.53	0
COL8A2	1.278	0.245	0.139	0.351	4.528	0
ZPLD1	1.162	0.15	0.085	0.215	4.527	0
LOC100272216	1.289	0.254	0.144	0.364	4.516	0
MCART6	1.481	0.393	0.222	0.564	4.514	0
MEI1	1.268	0.238	0.135	0.341	4.513	0
KCNS1	1.115	0.108	0.061	0.156	4.508	0
CYP2C9	1.146	0.137	0.077	0.196	4.501	0
SLCO5A1	1.32	0.278	0.156	0.399	4.479	0
PLCB2	1.39	0.33	0.185	0.474	4.471	0
CCL8	1.278	0.245	0.138	0.352	4.47	0
CXCR5	1.252	0.225	0.126	0.324	4.456	0
NUP210	1.494	0.401	0.225	0.578	4.454	0
TTC39C	1.434	0.36	0.201	0.519	4.438	0
ACAP1	1.31	0.27	0.15	0.389	4.433	0
LOC84740	1.143	0.133	0.074	0.192	4.43	0
ARRDC5	1.275	0.243	0.135	0.35	4.425	0
RLTPR	1.232	0.209	0.116	0.301	4.425	0
E2F2	1.378	0.321	0.178	0.464	4.394	0
SYTL1	1.249	0.222	0.123	0.321	4.393	0
CLIP4	1.31	0.27	0.15	0.391	4.391	0
FAM113B	1.425	0.354	0.196	0.513	4.374	0
GNA15	1.464	0.381	0.21	0.552	4.37	0
LILRB3	1.367	0.313	0.172	0.454	4.361	0
C2orf85	1.303	0.265	0.146	0.384	4.356	0
GLIPR2	1.572	0.453	0.249	0.656	4.355	0
GRIK4	1.175	0.162	0.089	0.234	4.355	0
KIAA1199	1.17	0.157	0.086	0.228	4.347	0
GMIP	1.559	0.444	0.243	0.645	4.332	0
FCRL5	1.149	0.139	0.076	0.202	4.319	0
ANGPTL3	0.882	-0.126	-0.183	-0.069	-4.31	0
BCL2A1	1.269	0.238	0.13	0.347	4.309	0
CTSZ	1.519	0.418	0.228	0.609	4.3	0
GPR109A	1.178	0.164	0.089	0.239	4.299	0
LOC96610	1.15	0.14	0.076	0.203	4.295	0
CRP	1.116	0.11	0.06	0.16	4.29	0
C19orf59	1.232	0.209	0.113	0.304	4.29	0
KIAA0125	1.177	0.163	0.089	0.238	4.288	0
PTPRN	1.112	0.107	0.058	0.155	4.286	0
AQP9	1.151	0.14	0.076	0.205	4.27	0
LYPD1	1.208	0.189	0.102	0.275	4.27	0
C17orf60	1.395	0.333	0.18	0.486	4.27	0
TYMP	1.416	0.347	0.187	0.508	4.256	0
CYSLTR1	0.76	-0.274	-0.401	-0.148	-4.253	0
VMO1	1.35	0.3	0.162	0.439	4.245	0
SP140	1.289	0.254	0.137	0.372	4.244	0
TRAF1	1.433	0.36	0.193	0.526	4.231	0
PITX2	1.112	0.106	0.057	0.155	4.23	0
TMEM45A	1.208	0.189	0.101	0.277	4.225	0

XCL2	1.253	0.226	0.121	0.33	4.216	0
DGKG	1.295	0.258	0.138	0.378	4.215	0
CARD9	1.344	0.296	0.158	0.434	4.196	0
WT1	1.125	0.118	0.063	0.172	4.194	0
CASP5	1.275	0.243	0.129	0.356	4.185	0
ZAP70	1.281	0.248	0.132	0.364	4.18	0
GPR172B	1.157	0.145	0.077	0.214	4.178	0
VENTX	1.327	0.283	0.15	0.416	4.178	0
PLB1	1.401	0.337	0.179	0.495	4.178	0
LOC100188949	1.288	0.253	0.134	0.372	4.176	0
MAN2B1	1.624	0.485	0.257	0.712	4.175	0
NMU	1.14	0.131	0.069	0.192	4.173	0
HIST1H2BG	1.216	0.196	0.104	0.288	4.172	0
APOBEC3H	1.291	0.255	0.135	0.375	4.171	0
EBI3	1.348	0.299	0.158	0.439	4.162	0
IBSP	1.137	0.128	0.068	0.189	4.16	0
RNASET2	1.25	0.223	0.117	0.329	4.132	0
CYTH4	1.418	0.349	0.183	0.515	4.129	0
GPR132	1.421	0.352	0.185	0.519	4.127	0
LIPA	0.684	-0.38	-0.561	-0.2	-4.126	0
FLT3LG	1.477	0.39	0.203	0.577	4.083	0
IL34	1.293	0.257	0.133	0.38	4.076	0
LAIR2	1.189	0.173	0.09	0.256	4.065	0
PSTPIP1	1.265	0.235	0.122	0.349	4.054	0
GBGT1	1.492	0.4	0.207	0.594	4.054	0
FCRL2	1.191	0.174	0.09	0.259	4.048	0
CCDC109B	1.366	0.312	0.161	0.463	4.04	0
TBC1D10C	1.279	0.246	0.126	0.365	4.036	0
FAP	1.215	0.195	0.1	0.289	4.033	0
ASCL2	1.283	0.249	0.128	0.37	4.03	0
ITGAX	1.322	0.279	0.143	0.415	4.025	0
MMP13	1.137	0.129	0.066	0.191	4.02	0
LILRA6	1.305	0.266	0.136	0.396	4.018	0
LAG3	1.166	0.154	0.079	0.229	4.015	0
XCL1	1.217	0.196	0.1	0.292	4.008	0
TNIP3	1.181	0.166	0.085	0.248	4.008	0
APOL1	1.224	0.202	0.103	0.301	4.001	0
TGFBI	1.136	0.128	0.065	0.19	3.994	0
C2orf89	1.195	0.178	0.091	0.266	3.989	0
PTPN7	1.263	0.233	0.119	0.348	3.988	0
GRAMD1B	1.277	0.245	0.124	0.365	3.981	0
ZBED2	1.162	0.15	0.076	0.224	3.955	0
ERC2	1.207	0.188	0.095	0.282	3.94	0
C20orf118	1.3	0.262	0.131	0.393	3.925	0
CFH	1.22	0.199	0.1	0.298	3.921	0
NTM	1.184	0.169	0.084	0.253	3.916	0
CSTA	1.33	0.285	0.142	0.428	3.913	0
GLT25D2	1.176	0.162	0.081	0.243	3.91	0
IL1R2	1.129	0.121	0.06	0.182	3.909	0
MAP4K1	1.262	0.233	0.116	0.349	3.907	0

SH3BP1	1.401	0.337	0.168	0.507	3.905	0
NEB	1.115	0.109	0.054	0.164	3.902	0
ADCY7	1.408	0.342	0.17	0.514	3.899	0
GREM1	1.115	0.109	0.054	0.163	3.891	0
WISP2	1.118	0.112	0.055	0.168	3.886	0
LILRB2	1.41	0.344	0.17	0.517	3.883	0
PARP15	1.227	0.205	0.101	0.308	3.882	0
ZNF683	1.211	0.191	0.095	0.288	3.882	0
LILRB1	1.417	0.349	0.172	0.525	3.879	0
CD14	1.345	0.296	0.146	0.446	3.874	0
TMPRSS13	1.217	0.196	0.097	0.295	3.871	0
ALOX12P2	1.176	0.162	0.08	0.244	3.871	0
LOC647121	1.345	0.296	0.146	0.447	3.87	0
CARD11	1.213	0.193	0.095	0.291	3.866	0
GBP2	1.399	0.336	0.165	0.506	3.865	0
TPSG1	1.109	0.104	0.051	0.156	3.863	0
STMN2	1.12	0.113	0.056	0.171	3.85	0
ICAM1	1.406	0.341	0.167	0.514	3.849	0
IFNG	1.161	0.15	0.073	0.226	3.847	0
SLC29A3	1.432	0.359	0.176	0.542	3.847	0
FHAD1	1.277	0.244	0.12	0.369	3.845	0
SPI1	1.368	0.313	0.154	0.473	3.845	0
FCGR1A	1.261	0.232	0.113	0.35	3.838	0
WNT10A	1.187	0.171	0.084	0.259	3.837	0
C1orf200	1.411	0.345	0.168	0.521	3.833	0
UGT2A3	0.915	-0.089	-0.135	-0.044	-3.83	0
SIGLEC1	1.266	0.236	0.115	0.357	3.824	0
ANKRD58	1.323	0.28	0.136	0.424	3.819	0
LGALS9C	1.339	0.292	0.142	0.442	3.811	0
CSF1	1.493	0.401	0.195	0.607	3.81	0
CECR6	1.378	0.321	0.156	0.486	3.81	0
CCL13	1.176	0.162	0.079	0.245	3.807	0
TTC24	1.212	0.192	0.093	0.291	3.804	0
PDPN	1.17	0.157	0.076	0.238	3.799	0
AGAP2	1.372	0.316	0.153	0.479	3.793	0
CSF3R	1.311	0.271	0.131	0.411	3.787	0
ARRB2	1.662	0.508	0.245	0.771	3.787	0
SPIB	1.193	0.177	0.085	0.269	3.784	0
PPYR1	1.185	0.169	0.081	0.258	3.772	0
RASGEF1C	1.136	0.128	0.061	0.194	3.772	0
FCER1G	1.346	0.297	0.142	0.452	3.765	0
APOBEC3G	1.337	0.291	0.139	0.442	3.763	0
CXCL6	1.102	0.097	0.046	0.148	3.758	0
IL18BP	1.451	0.372	0.178	0.566	3.758	0
WAS	1.343	0.295	0.141	0.45	3.747	0
LEF1	1.192	0.176	0.084	0.268	3.743	0
PSMB10	1.344	0.296	0.14	0.452	3.726	0
ZBTB32	1.273	0.241	0.114	0.368	3.719	0
KRT19	1.098	0.094	0.044	0.143	3.718	0
HLA-L	1.326	0.282	0.133	0.431	3.717	0

TNFAIP8L2	1.34	0.293	0.138	0.447	3.717	0
SH3KBP1	1.652	0.502	0.237	0.766	3.716	0
ATP1A3	1.138	0.129	0.061	0.197	3.715	0
RASAL3	1.385	0.326	0.154	0.498	3.713	0
SLFN14	1.288	0.253	0.119	0.386	3.712	0
HAS2	1.19	0.174	0.082	0.266	3.71	0
EMILIN2	1.418	0.349	0.165	0.533	3.708	0
GPR109B	1.161	0.149	0.07	0.229	3.694	0
POU2AF1	1.139	0.13	0.061	0.199	3.694	0
LOC606724	1.247	0.22	0.103	0.337	3.693	0
RNASE3	1.287	0.252	0.118	0.386	3.685	0
MICB	1.449	0.371	0.174	0.568	3.685	0
EMR4P	1.187	0.171	0.08	0.262	3.685	0
B3GAT1	1.195	0.178	0.083	0.273	3.682	0
HIVEP3	1.401	0.337	0.158	0.517	3.681	0
KIR2DL4	1.251	0.224	0.105	0.343	3.676	0
TCHH	1.163	0.151	0.07	0.232	3.667	0
TPRG1	1.187	0.171	0.08	0.263	3.664	0
AKR1B10	1.084	0.08	0.037	0.124	3.655	0
SPINK13	1.106	0.101	0.047	0.155	3.648	0
JAKMIP2	1.199	0.181	0.084	0.279	3.646	0
C1QL1	1.118	0.112	0.051	0.172	3.641	0
IDO2	1.261	0.232	0.107	0.356	3.641	0
C16orf74	1.149	0.139	0.064	0.214	3.638	0
CD82	1.278	0.245	0.113	0.377	3.636	0
IL2RA	1.182	0.167	0.077	0.257	3.634	0
DFNA5	1.336	0.29	0.133	0.447	3.63	0
LPPR4	1.19	0.174	0.08	0.269	3.625	0
S100A8	1.217	0.196	0.09	0.303	3.617	0
UCP2	1.32	0.278	0.127	0.429	3.609	0
TSPAN32	1.263	0.234	0.107	0.361	3.606	0
CDCP1	1.16	0.149	0.068	0.229	3.602	0
MYB	1.191	0.175	0.08	0.27	3.599	0
GLIPR1	1.314	0.273	0.124	0.423	3.589	0
CHRDL1	1.091	0.087	0.04	0.135	3.582	0
CIDEC	1.109	0.103	0.047	0.16	3.582	0
FGL2	0.79	-0.236	-0.366	-0.107	-3.578	0
IRF4	1.187	0.172	0.077	0.266	3.57	0
MYO1F	1.347	0.298	0.134	0.462	3.567	0
CD19	1.147	0.137	0.062	0.212	3.564	0
GXYLT2	1.151	0.141	0.063	0.218	3.564	0
GOLGA7B	1.177	0.163	0.073	0.253	3.563	0
IL21R	1.25	0.223	0.1	0.346	3.555	0
SPAG17	1.18	0.165	0.074	0.256	3.548	0
CLIC3	1.189	0.173	0.077	0.27	3.511	0
RAC2	1.281	0.248	0.109	0.386	3.511	0
VSIG4	1.235	0.211	0.093	0.329	3.509	0
NFATC2	0.847	-0.166	-0.259	-0.073	-3.503	0
PADI1	1.104	0.099	0.043	0.154	3.5	0
OPRL1	1.423	0.353	0.155	0.55	3.498	0

AXL	1.369	0.314	0.138	0.49	3.496	0
XCR1	0.832	-0.184	-0.287	-0.081	-3.49	0
LAIR1	1.309	0.269	0.118	0.42	3.485	0
C5orf46	1.087	0.083	0.036	0.13	3.484	0
CYP1B1	1.174	0.16	0.07	0.25	3.483	0
GJB2	1.175	0.162	0.071	0.252	3.483	0
CORO1A	1.291	0.255	0.111	0.399	3.478	0.001
GPR171	1.239	0.215	0.094	0.335	3.477	0.001
APOC2	1.145	0.135	0.059	0.211	3.476	0.001
CACNA2D4	1.221	0.2	0.087	0.312	3.473	0.001
CCL5	1.201	0.183	0.08	0.286	3.473	0.001
ADD2	1.151	0.141	0.061	0.221	3.464	0.001
C9orf139	1.22	0.199	0.086	0.312	3.457	0.001
LOC554202	1.126	0.119	0.052	0.187	3.456	0.001
SDC3	1.482	0.394	0.17	0.617	3.452	0.001
SERPINB9	1.467	0.383	0.165	0.601	3.449	0.001
LPXN	1.427	0.355	0.153	0.558	3.444	0.001
TSGA10IP	1.381	0.323	0.139	0.508	3.433	0.001
ADAM6	1.114	0.108	0.046	0.169	3.424	0.001
LGALS9	1.367	0.312	0.133	0.492	3.417	0.001
PDCD1	1.144	0.134	0.057	0.212	3.405	0.001
STAT4	1.336	0.29	0.123	0.457	3.402	0.001
LGALS12	1.104	0.099	0.042	0.156	3.393	0.001
PTGDS	1.133	0.124	0.053	0.196	3.391	0.001
PTPN6	1.501	0.406	0.171	0.641	3.388	0.001
LTA	1.209	0.19	0.08	0.3	3.387	0.001
MARCO	1.122	0.115	0.048	0.181	3.385	0.001
FAIM2	1.177	0.163	0.068	0.257	3.38	0.001
TLR2	1.328	0.284	0.119	0.449	3.374	0.001
GCNT1	1.244	0.218	0.091	0.345	3.365	0.001
SOD2	1.28	0.247	0.103	0.391	3.362	0.001
PLAC8	1.22	0.199	0.083	0.315	3.358	0.001
ODZ3	1.123	0.116	0.048	0.183	3.349	0.001
PVRIG	1.267	0.237	0.098	0.376	3.342	0.001
LHFPL2	1.313	0.273	0.113	0.433	3.339	0.001
PMCH	1.151	0.14	0.058	0.223	3.334	0.001
CD1E	0.85	-0.163	-0.259	-0.067	-3.321	0.001
SPINK1	1.084	0.081	0.033	0.129	3.315	0.001
SPOCK1	1.122	0.115	0.047	0.183	3.306	0.001
NLRC5	1.327	0.283	0.115	0.451	3.3	0.001
CD80	1.218	0.197	0.08	0.314	3.298	0.001
PTGDR	1.275	0.243	0.098	0.388	3.295	0.001
CFB	1.219	0.198	0.08	0.317	3.282	0.001
LILRA4	0.858	-0.153	-0.245	-0.062	-3.279	0.001
FBN2	1.171	0.158	0.063	0.252	3.278	0.001
KERA	1.215	0.194	0.078	0.311	3.273	0.001
MEFV	1.224	0.202	0.081	0.323	3.268	0.001
COMP	1.087	0.084	0.033	0.134	3.265	0.001
ITIH1	1.1	0.095	0.038	0.152	3.264	0.001
GHRL	1.249	0.223	0.089	0.356	3.261	0.001

LAT2	1.344	0.296	0.118	0.473	3.26	0.001
TRANK1	1.42	0.351	0.14	0.562	3.26	0.001
RGL4	1.255	0.227	0.09	0.364	3.259	0.001
KCND2	1.135	0.127	0.05	0.204	3.246	0.001
LTB	1.189	0.173	0.069	0.278	3.245	0.001
NCRNA00158	1.188	0.172	0.068	0.277	3.23	0.001
LOC400696	1.12	0.113	0.044	0.182	3.225	0.001
C1orf162	1.284	0.25	0.098	0.401	3.225	0.001
TNFSF13B	1.211	0.192	0.075	0.308	3.218	0.001
ADAP2	1.44	0.364	0.142	0.587	3.212	0.001
TNFSF11	1.138	0.129	0.05	0.208	3.209	0.001
PIK3CD	1.42	0.351	0.136	0.565	3.208	0.001
C1orf38	1.322	0.279	0.109	0.45	3.207	0.001
LAMP3	1.273	0.241	0.094	0.389	3.205	0.001
FMOD	1.144	0.134	0.052	0.217	3.204	0.001
FCER2	1.168	0.155	0.06	0.25	3.203	0.001
IL2RG	1.213	0.193	0.075	0.312	3.202	0.001
C20orf197	1.265	0.235	0.091	0.379	3.201	0.001
C2	1.143	0.134	0.052	0.216	3.198	0.001
C19orf38	1.3	0.262	0.101	0.423	3.195	0.001
LOC728875	1.199	0.182	0.07	0.293	3.194	0.001
TGM2	1.245	0.219	0.084	0.353	3.185	0.001
CLEC12B	1.206	0.188	0.072	0.303	3.185	0.001
DUSP10	1.313	0.272	0.104	0.44	3.178	0.001
SLC9A9	1.242	0.217	0.083	0.35	3.177	0.001
DUSP2	1.181	0.166	0.064	0.269	3.176	0.001
RYR1	1.232	0.208	0.08	0.337	3.175	0.001
PON3	1.132	0.124	0.047	0.201	3.171	0.002
SLAMF8	1.199	0.182	0.069	0.294	3.163	0.002
BATF3	1.25	0.223	0.085	0.361	3.161	0.002
LSP1	1.272	0.241	0.091	0.39	3.16	0.002
PATL2	1.193	0.177	0.067	0.286	3.157	0.002
CARD16	1.335	0.289	0.109	0.468	3.151	0.002
IFI30	1.261	0.232	0.087	0.377	3.138	0.002
CYP2S1	1.249	0.222	0.084	0.361	3.138	0.002
C15orf53	1.359	0.307	0.115	0.499	3.129	0.002
NNMT	1.197	0.18	0.067	0.293	3.123	0.002
IL9R	1.225	0.203	0.076	0.33	3.123	0.002
C6orf105	1.129	0.121	0.045	0.197	3.122	0.002
C13orf18	1.234	0.21	0.078	0.343	3.118	0.002
PSTPIP2	1.329	0.285	0.105	0.464	3.11	0.002
FAM26F	1.18	0.166	0.061	0.27	3.105	0.002
CCL19	1.09	0.086	0.031	0.141	3.079	0.002
TIGIT	1.161	0.15	0.054	0.245	3.075	0.002
LUM	1.098	0.094	0.034	0.153	3.072	0.002
PTHLH	1.088	0.085	0.031	0.139	3.071	0.002
GBP5	1.152	0.142	0.051	0.232	3.067	0.002
PTPN22	1.219	0.198	0.071	0.324	3.066	0.002
SFRP2	1.081	0.078	0.028	0.128	3.065	0.002
ALOX5	1.19	0.174	0.063	0.285	3.063	0.002

FERMT3	1.296	0.259	0.093	0.425	3.06	0.002
GFI1	1.201	0.183	0.066	0.301	3.058	0.002
CD300LB	1.255	0.227	0.081	0.372	3.053	0.002
KLRC3	1.191	0.175	0.062	0.287	3.05	0.002
FAM65B	0.835	-0.18	-0.296	-0.064	-3.046	0.002
MST4	1.254	0.226	0.081	0.372	3.045	0.002
SAMSN1	1.242	0.217	0.077	0.357	3.033	0.002
BLK	1.143	0.134	0.047	0.221	3.025	0.002
PNOC	1.142	0.132	0.047	0.218	3.021	0.003
KRT86	1.171	0.158	0.055	0.261	3.017	0.003
PTPRCAP	1.175	0.162	0.057	0.267	3.014	0.003
SLC35F3	1.117	0.111	0.039	0.183	3.008	0.003
TLR6	1.234	0.21	0.073	0.348	3.007	0.003
ENPP7	0.917	-0.087	-0.143	-0.03	-3.004	0.003
SERPING1	1.237	0.213	0.074	0.351	3.002	0.003
GZMH	1.196	0.179	0.062	0.295	2.999	0.003
GZMB	1.21	0.19	0.066	0.315	2.993	0.003
CD101	1.259	0.23	0.079	0.381	2.992	0.003
TP73	1.173	0.16	0.055	0.264	2.992	0.003
IL10RA	1.241	0.216	0.074	0.357	2.987	0.003
DSE	1.359	0.307	0.105	0.509	2.985	0.003
C8orf22	1.065	0.063	0.021	0.104	2.982	0.003
LST1	1.257	0.229	0.078	0.379	2.98	0.003
HMHA1	1.321	0.278	0.095	0.462	2.972	0.003
RGS1	1.193	0.176	0.06	0.293	2.971	0.003
MCOLN2	1.168	0.156	0.053	0.258	2.969	0.003
GAB3	1.36	0.308	0.104	0.511	2.967	0.003
APOC1	1.147	0.137	0.046	0.228	2.965	0.003
KMO	1.138	0.129	0.044	0.214	2.964	0.003
TFEC	0.881	-0.126	-0.21	-0.043	-2.964	0.003
CRYBB1	1.218	0.197	0.067	0.328	2.961	0.003
ITIH3	1.112	0.106	0.036	0.177	2.957	0.003
EMR1	1.167	0.154	0.052	0.256	2.955	0.003
NCF1B	1.197	0.18	0.06	0.299	2.948	0.003
CCL22	0.854	-0.157	-0.262	-0.052	-2.936	0.003
CEACAM21	1.233	0.209	0.07	0.349	2.935	0.003
TNFRSF17	1.125	0.118	0.039	0.196	2.934	0.003
IL24	1.293	0.257	0.085	0.429	2.926	0.003
C1QA	1.214	0.194	0.064	0.324	2.92	0.003
JAKMIP1	1.137	0.128	0.042	0.214	2.919	0.004
CCDC135	1.124	0.117	0.038	0.196	2.917	0.004
IL18RAP	1.211	0.192	0.063	0.32	2.915	0.004
TEX11	0.924	-0.079	-0.131	-0.026	-2.906	0.004
HTRA4	1.13	0.122	0.04	0.204	2.902	0.004
SEMA4A	1.267	0.236	0.076	0.396	2.895	0.004
GNB4	1.36	0.307	0.099	0.515	2.894	0.004
THBS2	1.124	0.117	0.038	0.196	2.89	0.004
SLA2	1.182	0.168	0.054	0.281	2.89	0.004
TRAF3IP3	1.219	0.198	0.064	0.332	2.887	0.004
AIF1	1.271	0.24	0.077	0.403	2.88	0.004

KLRK1	1.179	0.165	0.052	0.277	2.876	0.004
BCL2L14	1.215	0.195	0.062	0.328	2.872	0.004
SIGLEC12	1.126	0.119	0.038	0.2	2.871	0.004
AKNA	1.308	0.269	0.085	0.452	2.862	0.004
CD1C	0.863	-0.147	-0.248	-0.046	-2.861	0.004
ELFN2	1.094	0.089	0.028	0.151	2.858	0.004
C3	1.149	0.139	0.043	0.235	2.843	0.004
TNNI2	1.188	0.172	0.053	0.292	2.827	0.005
MMP7	1.088	0.084	0.026	0.142	2.827	0.005
LRG1	1.116	0.11	0.034	0.186	2.826	0.005
LPAR6	1.298	0.261	0.08	0.442	2.825	0.005
CCR3	1.23	0.207	0.063	0.351	2.823	0.005
EMB	1.244	0.218	0.067	0.369	2.821	0.005
IL2RB	1.209	0.19	0.058	0.321	2.821	0.005
ST18	1.211	0.192	0.058	0.325	2.819	0.005
CD79A	1.11	0.105	0.032	0.178	2.814	0.005
RASGEF1A	1.154	0.143	0.043	0.243	2.805	0.005
APOH	1.078	0.075	0.023	0.128	2.798	0.005
VSIG1	1.14	0.131	0.039	0.222	2.793	0.005
LAMB3	1.106	0.101	0.03	0.171	2.782	0.005
C1orf127	1.216	0.196	0.058	0.334	2.775	0.006
MYO1G	1.201	0.183	0.054	0.313	2.774	0.006
ST8SIA1	1.16	0.149	0.044	0.254	2.773	0.006
CLEC4D	1.196	0.179	0.052	0.306	2.769	0.006
SIRPG	1.127	0.12	0.035	0.205	2.761	0.006
CHRDL2	1.084	0.081	0.023	0.138	2.76	0.006
TNFRSF1B	1.34	0.293	0.084	0.501	2.754	0.006
ZMYND15	1.281	0.247	0.071	0.424	2.747	0.006
STAT5A	1.386	0.327	0.093	0.56	2.745	0.006
OLFML3	1.233	0.21	0.06	0.36	2.744	0.006
APOE	1.161	0.149	0.043	0.256	2.74	0.006
EMR2	1.229	0.206	0.058	0.354	2.735	0.006
FCGR3A	1.194	0.177	0.05	0.304	2.723	0.006
CD97	1.38	0.322	0.09	0.554	2.722	0.006
ENKUR	1.156	0.145	0.041	0.249	2.721	0.007
NPTX2	1.087	0.083	0.023	0.144	2.717	0.007
ANKRD22	1.121	0.114	0.032	0.196	2.714	0.007
RASSF5	1.251	0.224	0.062	0.386	2.713	0.007
TNFRSF13B	1.145	0.135	0.037	0.233	2.708	0.007
MUC13	1.091	0.087	0.024	0.15	2.707	0.007
VPREB3	1.162	0.15	0.041	0.259	2.705	0.007
FASLG	1.14	0.131	0.036	0.226	2.7	0.007
NALCN	1.104	0.099	0.027	0.17	2.697	0.007
TXLNB	1.184	0.169	0.046	0.292	2.696	0.007
CCR8	1.154	0.143	0.039	0.248	2.693	0.007
ICAM3	1.318	0.276	0.075	0.477	2.693	0.007
SSTR3	1.288	0.253	0.069	0.438	2.692	0.007
S100B	1.152	0.141	0.038	0.244	2.686	0.007
EVI2A	1.228	0.205	0.055	0.355	2.686	0.007
APOBEC3A	1.198	0.18	0.048	0.312	2.68	0.007

SYT12	1.101	0.096	0.026	0.167	2.667	0.008
FN1	1.18	0.165	0.044	0.287	2.663	0.008
CADM3	1.082	0.079	0.021	0.137	2.662	0.008
ASGR2	1.155	0.144	0.038	0.25	2.661	0.008
TYROBP	1.222	0.201	0.053	0.349	2.656	0.008
NAIP	1.218	0.197	0.052	0.343	2.652	0.008
ARX	1.082	0.079	0.02	0.137	2.65	0.008
GZMM	1.189	0.173	0.045	0.301	2.65	0.008
TMEM150B	1.19	0.174	0.045	0.302	2.649	0.008
GPR18	1.179	0.165	0.043	0.287	2.642	0.008
CXCR4	1.259	0.231	0.059	0.402	2.64	0.008
PLA2G2D	1.092	0.088	0.022	0.153	2.637	0.008
C2orf65	1.212	0.192	0.049	0.336	2.63	0.009
SCRG1	1.099	0.094	0.024	0.164	2.63	0.009
TRIM54	1.072	0.069	0.018	0.121	2.628	0.009
TMC6	1.336	0.29	0.073	0.506	2.625	0.009
CD37	1.235	0.211	0.053	0.369	2.623	0.009
NINJ2	1.208	0.189	0.048	0.331	2.622	0.009
LAPTM5	1.243	0.218	0.055	0.38	2.621	0.009
B3GALT5	1.092	0.088	0.022	0.154	2.619	0.009
CXCR3	1.132	0.124	0.031	0.217	2.616	0.009
TNFSF12-TNFSF13	1.145	0.136	0.034	0.237	2.614	0.009
TREM2	1.177	0.163	0.041	0.285	2.61	0.009
PLCXD2	1.211	0.191	0.047	0.336	2.6	0.009
KIF21B	1.205	0.186	0.046	0.326	2.6	0.009
FGA	1.049	0.048	0.012	0.084	2.587	0.01
SPIC	0.836	-0.18	-0.316	-0.043	-2.583	0.01
ISLR	1.096	0.092	0.022	0.161	2.58	0.01
CCL4	1.162	0.15	0.036	0.264	2.577	0.01
IL1B	1.155	0.144	0.034	0.253	2.575	0.01
TTLL6	1.105	0.1	0.023	0.176	2.56	0.01
SIRPB2	1.221	0.199	0.046	0.352	2.556	0.011
DNASE2B	0.874	-0.135	-0.238	-0.031	-2.551	0.011
CTSE	0.918	-0.085	-0.151	-0.02	-2.548	0.011
SPNS3	1.154	0.143	0.033	0.253	2.543	0.011
ADRBK2	1.35	0.3	0.068	0.532	2.536	0.011
FUT7	1.193	0.176	0.04	0.312	2.532	0.011
C1QB	1.174	0.16	0.036	0.285	2.528	0.011
NLRP7	1.175	0.161	0.036	0.286	2.527	0.011
C11orf21	1.177	0.163	0.036	0.29	2.523	0.012
CFD	1.15	0.14	0.031	0.249	2.516	0.012
KCNK6	1.237	0.213	0.047	0.379	2.513	0.012
SIGLEC11	1.153	0.142	0.031	0.253	2.509	0.012
GTSF1L	1.17	0.157	0.034	0.28	2.508	0.012
CD300A	1.201	0.183	0.04	0.327	2.505	0.012
CD52	1.189	0.173	0.037	0.309	2.5	0.012
KCNAB2	1.212	0.193	0.042	0.344	2.5	0.012
GBP6	1.173	0.16	0.034	0.285	2.493	0.013
C12orf36	1.059	0.057	0.012	0.102	2.49	0.013
FPR2	1.15	0.139	0.029	0.25	2.473	0.013

C5AR1	1.207	0.189	0.039	0.338	2.473	0.013
SIGLEC10	1.186	0.171	0.035	0.306	2.473	0.013
VCAN	1.128	0.121	0.025	0.216	2.472	0.013
CKM	1.179	0.164	0.034	0.295	2.469	0.014
FCGR2A	1.239	0.214	0.044	0.385	2.467	0.014
SELPLG	1.24	0.215	0.044	0.386	2.467	0.014
TTC16	1.163	0.151	0.031	0.271	2.465	0.014
PRR5L	1.26	0.231	0.047	0.416	2.457	0.014
BIN2	1.24	0.215	0.044	0.387	2.457	0.014
DOK2	1.223	0.202	0.041	0.363	2.454	0.014
CD27	1.107	0.102	0.02	0.184	2.443	0.015
SLAMF1	1.157	0.146	0.029	0.263	2.438	0.015
CD6	1.166	0.154	0.03	0.277	2.437	0.015
CX3CR1	0.89	-0.116	-0.21	-0.022	-2.43	0.015
IL10	1.15	0.14	0.027	0.253	2.425	0.015
RIMBP3	1.226	0.204	0.039	0.369	2.421	0.015
LOC100233209	1.167	0.155	0.029	0.28	2.421	0.015
TNS4	1.115	0.109	0.02	0.198	2.4	0.016
S100A9	1.144	0.135	0.024	0.245	2.393	0.017
RIPK3	1.283	0.249	0.045	0.453	2.392	0.017
SFMBT2	0.869	-0.141	-0.256	-0.025	-2.391	0.017
STAG3	1.165	0.153	0.027	0.278	2.389	0.017
ME1	1.18	0.165	0.03	0.301	2.387	0.017
ZNF804A	1.172	0.159	0.028	0.29	2.384	0.017
ARNTL2	1.172	0.158	0.028	0.289	2.377	0.017
GAL3ST4	1.189	0.173	0.03	0.315	2.375	0.018
LGI4	1.081	0.078	0.013	0.143	2.361	0.018
ECEL1	1.085	0.082	0.014	0.149	2.357	0.018
ICOS	1.121	0.114	0.019	0.21	2.354	0.019
CR1	1.115	0.109	0.018	0.199	2.352	0.019
CCL3	1.13	0.122	0.02	0.224	2.351	0.019
FCGR2C	1.152	0.142	0.023	0.26	2.347	0.019
SASH3	1.196	0.179	0.029	0.328	2.345	0.019
KLRC1	1.138	0.129	0.021	0.237	2.344	0.019
C11orf86	1.076	0.073	0.012	0.135	2.343	0.019
POSTN	1.115	0.109	0.018	0.2	2.343	0.019
SECTM1	1.169	0.156	0.025	0.287	2.336	0.02
CD3E	1.128	0.121	0.019	0.222	2.334	0.02
AMPD1	1.117	0.111	0.017	0.205	2.319	0.02
HLA-G	0.911	-0.093	-0.171	-0.014	-2.317	0.02
SAMD3	1.165	0.153	0.023	0.283	2.314	0.021
GSTA2	0.95	-0.052	-0.095	-0.008	-2.311	0.021
S100A4	1.194	0.177	0.027	0.327	2.308	0.021
ANKRD44	0.852	-0.16	-0.295	-0.024	-2.308	0.021
CLEC9A	0.895	-0.111	-0.206	-0.017	-2.307	0.021
UBASH3A	1.116	0.11	0.016	0.203	2.305	0.021
SYNGR3	1.087	0.083	0.012	0.155	2.284	0.022
S100Z	1.203	0.185	0.026	0.344	2.279	0.023
KLRC4	1.116	0.11	0.015	0.204	2.275	0.023
CCR4	0.9	-0.106	-0.197	-0.015	-2.273	0.023

PTCRA	1.203	0.185	0.025	0.344	2.271	0.023
FAM159A	1.167	0.154	0.021	0.287	2.27	0.023
P2RX1	1.139	0.13	0.018	0.243	2.266	0.023
VAV1	1.175	0.162	0.022	0.302	2.262	0.024
DNAJB13	1.067	0.065	0.009	0.121	2.258	0.024
SAMD9L	1.194	0.177	0.023	0.331	2.253	0.024
TMIGD2	1.159	0.148	0.019	0.277	2.245	0.025
C1QC	1.159	0.147	0.019	0.276	2.245	0.025
CTSW	1.128	0.12	0.015	0.226	2.244	0.025
TAP1	1.269	0.238	0.03	0.446	2.244	0.025
TRPC2	1.069	0.067	0.008	0.126	2.243	0.025
IRF1	1.216	0.196	0.024	0.367	2.236	0.025
CCR1	1.157	0.146	0.018	0.274	2.229	0.026
BEND4	1.139	0.13	0.015	0.245	2.224	0.026
PSMB9	1.215	0.195	0.023	0.366	2.222	0.026
TCF7	1.171	0.158	0.018	0.298	2.217	0.027
XKR9	1.125	0.118	0.013	0.222	2.208	0.027
GPR25	1.226	0.204	0.022	0.386	2.199	0.028
TNFSF9	1.125	0.117	0.013	0.222	2.198	0.028
SLC34A2	1.047	0.046	0.005	0.087	2.192	0.028
NKG7	1.122	0.115	0.012	0.217	2.191	0.028
NFAM1	1.208	0.189	0.019	0.358	2.185	0.029
GPR133	1.116	0.11	0.011	0.209	2.184	0.029
TMEM92	1.069	0.067	0.007	0.127	2.182	0.029
SIRPD	1.197	0.18	0.018	0.341	2.182	0.029
FAM49B	1.32	0.278	0.028	0.527	2.182	0.029
C8orf80	0.915	-0.088	-0.168	-0.009	-2.18	0.029
HLA-DQB2	0.904	-0.101	-0.191	-0.01	-2.176	0.03
SIGLEC9	1.177	0.163	0.016	0.311	2.172	0.03
GTSF1	1.115	0.109	0.011	0.208	2.17	0.03
FAM78A	1.219	0.198	0.019	0.377	2.17	0.03
C21orf7	1.142	0.133	0.013	0.253	2.167	0.03
MPO	1.113	0.107	0.01	0.204	2.158	0.031
PRAM1	1.169	0.156	0.014	0.298	2.155	0.031
LTF	0.937	-0.065	-0.124	-0.006	-2.155	0.031
TMEM119	1.104	0.099	0.009	0.189	2.15	0.032
OAS2	1.222	0.2	0.018	0.383	2.148	0.032
BIRC3	1.146	0.137	0.012	0.261	2.147	0.032
MOXD1	1.084	0.08	0.007	0.154	2.147	0.032
FABP6	1.081	0.078	0.007	0.149	2.144	0.032
PADI2	1.132	0.124	0.01	0.238	2.138	0.032
TRPV2	1.29	0.254	0.021	0.488	2.136	0.033
C19orf21	1.064	0.062	0.005	0.119	2.134	0.033
CP	1.062	0.061	0.005	0.116	2.134	0.033
CD33	1.186	0.171	0.013	0.328	2.125	0.034
FCGR2B	1.125	0.118	0.009	0.227	2.122	0.034
SLC15A3	1.203	0.184	0.014	0.355	2.116	0.034
STAT1	1.19	0.174	0.012	0.335	2.104	0.035
HCK	1.2	0.182	0.012	0.352	2.1	0.036

CLEC5A	1.131	0.123	0.008	0.238	2.098	0.036
CST7	1.115	0.109	0.007	0.211	2.093	0.036
FGD3	1.183	0.168	0.011	0.326	2.093	0.036
FCRLA	1.099	0.094	0.006	0.183	2.09	0.037
GPR114	1.16	0.148	0.009	0.287	2.089	0.037
GZMA	1.117	0.11	0.007	0.214	2.083	0.037
MGC45800	1.076	0.073	0.004	0.142	2.075	0.038
F13A1	1.105	0.1	0.005	0.194	2.074	0.038
LOX	1.087	0.083	0.004	0.162	2.072	0.038
AKAP5	1.161	0.149	0.008	0.291	2.071	0.038
GIMAP4	0.836	-0.179	-0.348	-0.009	-2.07	0.038
COTL1	1.256	0.228	0.012	0.445	2.066	0.039
CEBPA	1.136	0.127	0.006	0.248	2.062	0.039
SLAMF6	1.117	0.111	0.005	0.216	2.061	0.039
HLA-DOB	1.098	0.094	0.004	0.183	2.055	0.04
CHI3L1	1.082	0.079	0.004	0.154	2.054	0.04
CLEC17A	1.111	0.105	0.005	0.206	2.052	0.04
GPR35	1.081	0.078	0.003	0.153	2.052	0.04
SIT1	1.105	0.1	0.004	0.195	2.049	0.04
NCF1	1.139	0.131	0.005	0.256	2.046	0.041
C6orf97	1.15	0.139	0.006	0.273	2.042	0.041
SCML4	1.138	0.129	0.005	0.253	2.039	0.041
CPVL	0.887	-0.12	-0.235	-0.004	-2.036	0.042
RPGRIP1	1.173	0.16	0.006	0.314	2.031	0.042
RHOH	1.138	0.13	0.004	0.255	2.03	0.042
ITGAL	1.139	0.13	0.004	0.256	2.026	0.043
PILRA	1.186	0.171	0.005	0.337	2.017	0.044
ARL11	1.203	0.185	0.005	0.364	2.015	0.044
ASB2	1.114	0.108	0.003	0.214	2.007	0.045
BMF	1.221	0.2	0.004	0.395	2.004	0.045
BCL11B	1.129	0.122	0.003	0.241	2.003	0.045
MGAT3	1.106	0.1	0.002	0.199	2	0.046
RFPL1S	1.139	0.131	0.003	0.258	1.999	0.046
MFAP5	1.068	0.066	0.001	0.131	1.996	0.046
PPP2R2B	1.139	0.13	0.002	0.258	1.991	0.046
S100A1	1.067	0.065	0.001	0.13	1.989	0.047
IL12RB1	1.145	0.135	0.002	0.268	1.984	0.047
P2RY12	0.912	-0.093	-0.184	-0.001	-1.983	0.047
IPCEF1	0.864	-0.147	-0.292	-0.002	-1.982	0.047
CD3D	1.101	0.097	0.001	0.192	1.981	0.048
CLRN3	0.947	-0.054	-0.108	0	-1.974	0.048
GCM1	1.089	0.086	0	0.171	1.964	0.05
FLT3	0.909	-0.095	-0.19	0	-1.963	0.05
PRIMA1	1.049	0.048	0	0.096	1.96	0.05

Table S2. Each protein's extracellular/subcellular locations in PPI network

PPI network	Protein	Extracellular/Subcellular location	Predicted location
Module 1	ADCY7	Cytosol	Intracellular, Membrane (different isoforms)
Module 1	C5AR1	Vesicles	Intracellular, Membrane (different isoforms)
Module 1	CCL13	Secreted to blood	Intracellular, Secreted (different isoforms)
Module 1	CCL13	Secreted to blood	Intracellular, Secreted (different isoforms)
Module 1	CCL19	Secreted to blood	Secreted
Module 1	CCL4	Secreted to blood	Secreted
Module 1	CCL5	Secreted to blood	Membrane, Secreted (different isoforms)
Module 1	CCR1	-	Membrane
Module 1	CCR3	-	Intracellular, Membrane (different isoforms)
Module 1	CCR8	-	Intracellular, Membrane (different isoforms)
Module 1	CXCL1	Secreted to blood	Secreted
Module 1	CXCL13	Secreted to blood	Secreted
Module 1	CXCL5	Secreted to blood	Secreted
Module 1	CXCL6	Secreted to blood	Secreted
Module 1	CXCL8	Secreted to blood	Secreted
Module 1	CXCR3	-	Membrane
Module 1	CXCR4	-	Membrane
Module 1	CXCR5	-	Membrane
Module 1	FPR2	-	Membrane
Module 1	GNB4	Plasma membrane	Intracellular
Module 1	GPR18	-	Membrane
Module 1	GPSM3	-	Intracellular
Module 1	HCAR2	Cell Junctions	Membrane
Module 1	HCAR3	Cell Junctions	Membrane
Module 1	NMU	Locally secreted	Secreted
Module 1	NPY4R	-	Membrane
Module 1	OPRL1	-	Membrane
Module 1	PMCH	Secreted to blood	Secreted
Module 1	PNOC	Secreted to blood	Intracellular, Secreted (different isoforms)
Module 1	S1PR2	-	Membrane
Module 1	SAA1	Secreted to blood	Secreted
Module 1	SSTR3	-	Membrane
Module 2	TACC3	Mitotic spindle, Centriolar satellite, Cytosol and additionally in Vesicles	Intracellular
Module 2	ASPM	Plasma membrane, Cytosol	Intracellular
Module 2	AURKB	Nucleoplasm, Midbody	Intracellular
Module 2	BIRC5	Cytokinetic bridge	Intracellular
Module 2	CCL3	Secreted to blood	Secreted
Module 2	CENPA	Nucleoplasm	Intracellular
Module 2	CEP55	Plasma membrane, Centriolar satellite and additionally in Midbody	Intracellular
Module 2	CKAP2L	Mitotic spindle and additionally in Cytosol	Intracellular
Module 2	CTLA4	-	Intracellular, Membrane (different isoforms)
Module 2	DLGAP5	Centriolar satellite, Cytosol	Intracellular
Module 2	FASLG	Secreted to blood	Membrane, Secreted (different isoforms)
Module 2	FCGR2B	-	Membrane
Module 2	FN1	Secreted to blood	Intracellular, Secreted (different isoforms)
Module 2	FOXP3	Nucleoplasm	Intracellular
Module 2	HJURP	Nucleoplasm, Nucleoli and additionally in Mitochondria	Intracellular
Module 2	IL10	Secreted to blood	Intracellular, Secreted (different isoforms)
Module 2	IL2RA	-	Intracellular, Membrane (different isoforms)
Module 2	IL6	Vesicles	Intracellular, Secreted (different isoforms)
Module 2	ITGAL	-	Intracellular, Membrane (different isoforms)
Module 2	ITGAX	-	Intracellular, Membrane (different isoforms)
Module 2	KIF14	Cytosol and additionally in Midbody ring	Intracellular
Module 2	KIF15	-	Intracellular
Module 2	KIF2C	Nucleoplasm, Centrosome and additionally in Midbody	Intracellular
Module 2	MKI67	Nucleoplasm, Nucleoli	Intracellular

Module 2	MYBL2	Nucleoplasm and additionally in Cytosol	Intracellular
Module 2	NCAPG	-	Intracellular
Module 2	NCAPH	Cytosol and additionally in Nucleoplasm	Intracellular
Module 2	CENPE	Microtubules, Cytosol and additionally in Nucleoplasm	Intracellular
Module 2	SGOL1	Nucleoplasm and additionally in Nuclear bodies, Cytosol	Intracellular
Module 2	PTTG1	Cytosol and additionally in Nucleoli	Intracellular
Module 2	RRM2	Cytosol	Intracellular, Membrane (different isoforms)
Module 2	SHCBP1	Nuclear bodies and additionally in Microtubules, Midbody, Mitotic spindle	Intracellular
Module 2	TLR6	Endoplasmic reticulum	Membrane
Module 2	TNFRSF1B	Secreted to blood	Membrane, Secreted (different isoforms)
Module 2	UBE2C	Plasma membrane, Cytosol	Intracellular
Module 2	NUF2	Nucleoplasm	Intracellular
Module 2	UHRF1	Nucleoplasm	Intracellular
Module 3	ADAM8	-	Intracellular, Membrane (different isoforms)
Module 3	APOE	Secreted to blood/Vesicles	Secreted
Module 3	CCL8	Secreted to blood	Secreted
Module 3	CD27	-	Membrane
Module 3	CD300A	-	Intracellular, Membrane (different isoforms)
Module 3	CD3E	-	Membrane
Module 3	CD80	-	Membrane
Module 3	CLEC4D	-	Intracellular
Module 3	CLEC5A	Plasma membrane, Cytosol	Intracellular, Membrane (different isoforms)
Module 3	CRP	Secreted to blood	Intracellular, Secreted (different isoforms)
Module 3	CYBA	-	Intracellular, Membrane (different isoforms)
Module 3	FCER1G	-	Membrane
Module 3	FCGR2A	Plasma membrane and additionally in Golgi apparatus	Intracellular, Membrane (different isoforms)
Module 3	GPR84	-	Membrane
Module 3	GZMA	Secreted to blood	Secreted
Module 3	ICOS	Plasma membrane and additionally in Actin filaments	Membrane
Module 3	IL10RA	-	Membrane
Module 3	IL12RB1	Plasma membrane	Intracellular, Membrane (different isoforms)
Module 3	IL1RN	Secreted to blood/Nucleoplasm and additionally in Centrosome, Cytosol	Intracellular, Secreted (different isoforms)
Module 3	IL21R	Plasma membrane, Cytosol	Membrane
Module 3	IL2RG	Vesicles	Intracellular, Membrane (different isoforms)
Module 3	IRF4	Nucleoplasm and additionally in Cytosol	Intracellular
Module 3	JAK3	Plasma membrane, Cytosol	Intracellular
Module 3	KCNAB2	-	Intracellular
Module 3	LAG3	Secreted-unknown location	Membrane, Secreted (different isoforms)
Module 3	LAIR1	Plasma membrane	Intracellular, Membrane (different isoforms)
Module 3	LILRB2	-	Membrane
Module 3	LMNB1	Nuclear membrane	Intracellular
Module 3	MCEMP1	-	Membrane
Module 3	MMP9	Secreted to blood/Cytosol	Secreted
Module 3	MPO	Vesicles and additionally in Nucleoplasm	Intracellular
Module 3	NOD2	Golgi apparatus, Cytosol	Intracellular
Module 3	P2RX1	-	Membrane
Module 3	PDCD1	-	Intracellular, Membrane (different isoforms)
Module 3	PLAUR	Plasma membrane	Intracellular, Membrane (different isoforms)
Module 3	SLC11A1	-	Membrane
Module 3	STAT1	Nucleoplasm, Cytosol	Intracellular
Module 3	STAT4	-	Intracellular
Module 3	STAT5A	Nucleoplasm, Cytosol	Intracellular
Module 3	TMC6	-	Intracellular, Membrane (different isoforms)
Module 3	TNFRSF18	Secreted to blood	Membrane, Secreted (different isoforms)
Module 3	TNFSF4	Nucleoplasm, Vesicles	Intracellular
Module 3	TRPM2	Nuclear membrane	Intracellular, Membrane (different isoforms)
Module 3	XCL2	Secreted to blood	Secreted
Module 3	ZAP70	-	Intracellular

Table S3. Comparison of mRNA expression between carcinoma and normal tissue in Oncomine database

Genes	Clear Cell Renal Carcinoma vs. Normal			
	Number of cases	Cohort	Fold Change	*P* value
AIF1	Carcinoma: 27; Normal: 11	Beroukhim Renal	1.266	0.094
	Carcinoma: 10; Normal: 10	Gumz Renal	1.827	0.012
	Carcinoma: 3; Normal: 25	Higgins Renal	1.151	0.382
	Carcinoma: 23; Normal: 23	Jones Renal	1.866	0.000
	Carcinoma: 9; Normal: 9	Lenburg Renal	1.27	0.030
	Carcinoma: 26; Normal: 5	Yusenko Renal	2.818	0.000
FCER1G	Carcinoma: 27; Normal: 11	Beroukhim Renal	6.293	0.000
	Carcinoma: 10; Normal: 10	Gumz Renal	3.246	0.000
	Carcinoma: 23; Normal: 23	Jones Renal	2.48	0.000
	Carcinoma: 9; Normal: 9	Lenburg Renal	3.108	0.000
	Carcinoma: 26; Normal: 5	Yusenko Renal	10.501	0.000
IL10RA	Carcinoma: 27; Normal: 11	Beroukhim Renal	5.265	0.000
	Carcinoma: 10; Normal: 10	Gumz Renal	4.215	0.000
	Carcinoma: 23; Normal: 23	Jones Renal	2.65	0.000
	Carcinoma: 9; Normal: 9	Lenburg Renal	2.279	0.000
	Carcinoma: 26; Normal: 5	Yusenko Renal	6.728	0.000
IL12RB1	Carcinoma: 27; Normal: 11	Beroukhim Renal	1.095	0.025
	Carcinoma: 23; Normal: 23	Jones Renal	-2.758	1.000
	Carcinoma: 9; Normal: 9	Lenburg Renal	1.096	0.076
	Carcinoma: 26; Normal: 5	Yusenko Renal	4.593	0.007
LAPTM5	Carcinoma: 26; Normal: 5	Yusenko Renal	10.501	0.000
	Carcinoma: 27; Normal: 11	Beroukhim Renal	6.293	0.000
	Carcinoma: 10; Normal: 10	Gumz Renal	5.585	0.000
	Carcinoma: 23; Normal: 23	Jones Renal	2.993	0.000
	Carcinoma: 9; Normal: 9	Lenburg Renal	4.27	0.000
LPXN	Carcinoma: 20; Normal: 3	Higgins Renal	-1.059	0.651
RHOH	Carcinoma: 27; Normal: 11	Beroukhim Renal	1.778	0.000
	Carcinoma: 10; Normal: 10	Gumz Renal	3.765	0.000
	Carcinoma: 23; Normal: 23	Jones Renal	1.121	0.003
	Carcinoma: 9; Normal: 9	Lenburg Renal	1.212	0.068
	Carcinoma: 26; Normal: 5	Yusenko Renal	20.809	0.000
SASH3	Carcinoma: 27; Normal: 11	Beroukhim Renal	2.094	0.000
	Carcinoma: 10; Normal: 10	Gumz Renal	1.552	0.001
	Carcinoma: 23; Normal: 23	Jones Renal	1.445	0.000
	Carcinoma: 9; Normal: 9	Lenburg Renal	1.745	0.000
	Carcinoma: 26; Normal: 5	Yusenko Renal	3.623	0.000
SP140	Carcinoma: 27; Normal: 11	Beroukhim Renal	1.242	0.002
	Carcinoma: 10; Normal: 10	Gumz Renal	2.894	0.000
	Carcinoma: 23; Normal: 23	Jones Renal	1.188	0.015
	Carcinoma: 9; Normal: 9	Lenburg Renal	1.113	0.106
	Carcinoma: 26; Normal: 5	Yusenko Renal	3.523	0.038
TIGIT	Carcinoma: 10; Normal: 10	Gumz Renal	1.021	0.463
	Carcinoma: 9; Normal: 9	Lenburg Renal	1.077	0.116
	Carcinoma: 26; Normal: 5	Yusenko Renal	7.749	0.001

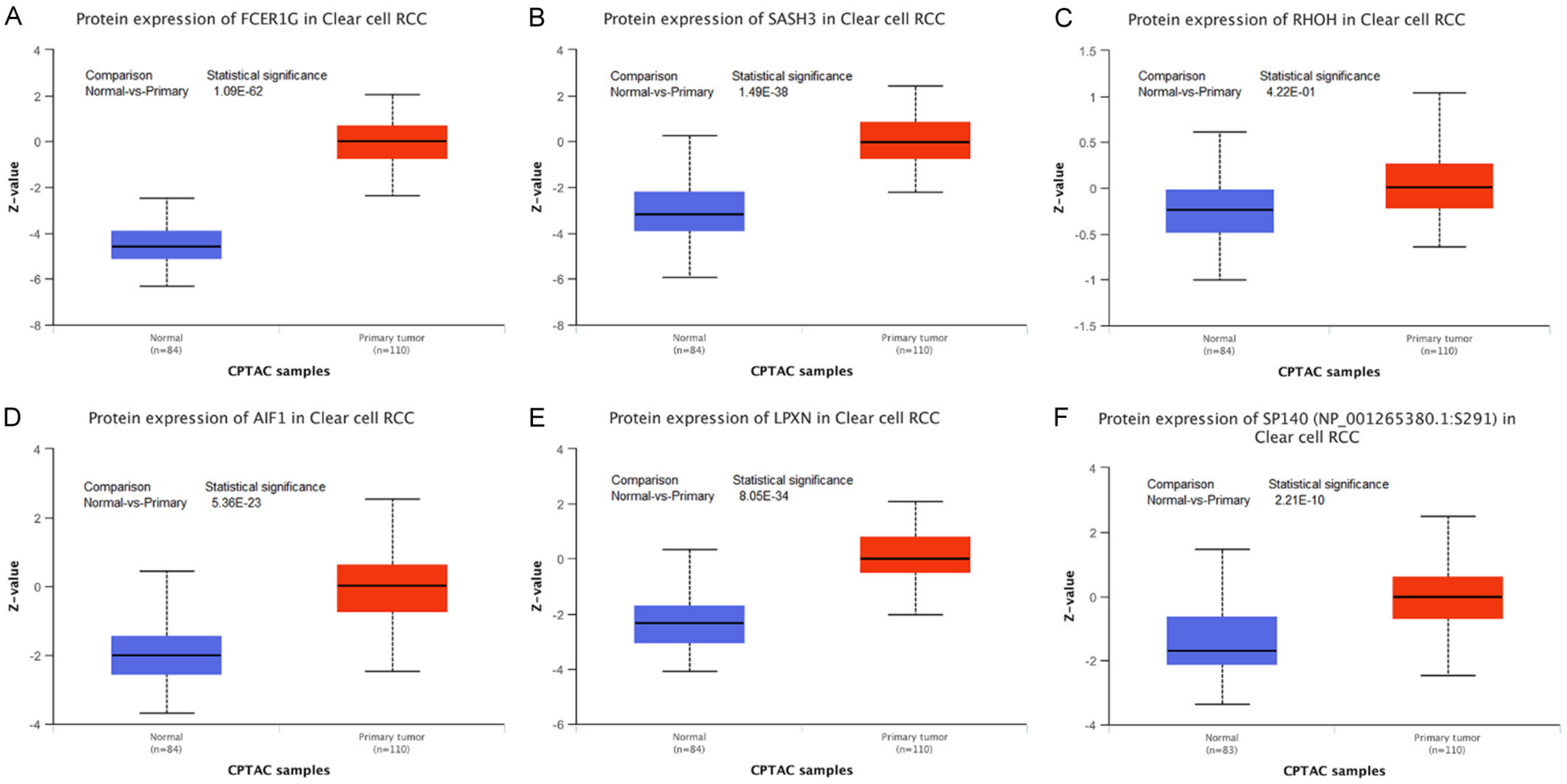

Figure S1. Comparison of protein expression between carcinoma and normal tissue in CPTAC database. (A-F) Represented the protein expression of FCER1G, SASH3, RHOH, AIF1, LPXN and SP140 between carcinoma and normal tissue, respectively. Except for RHOH (C), all proteins were differentially expressed between carcinoma and normal tissue (*P* value < 0.05).